ABSTRACT

NADKARNI, AKSHAY NITISH. Designing a Next-Generation Antibody Purification Process by Integrating a Decoupling Precipitation Capture Step. (Under the direction of Dr. Ruben Carbonell, Dr. Gary Gilleskie, and Dr. Baley Reeves.)

Recent breakthroughs in mammalian cell culture processes for the production of monoclonal antibody (mAb) products have yielded upstream processes with product titers of five grams per liter or greater. It is predicted that upstream processes will reach the ten gram per liter titer mark in the near future. Traditional downstream purification processes, which utilize Protein A affinity chromatography as a primary product capture step, face significant bottlenecks in the face of this increase in incoming product. The work presented in this thesis aims to design a next-generation, non-Protein A antibody purification process that integrates a protein precipitation technology for decoupling upstream and downstream processing. This next-generation process will utilize an existing polyethylene glycol (PEG)/zinc chloride precipitation technology in order to capture and store product from incoming cell culture harvest. Antibody product in this precipitated form is stable and can be stored at -70 ^{O}C, removing the need for immediate product purification and effectively 'decoupling' upstream and downstream processing for antibody products. Elimination of the Protein A capture step, along with implementation of PEG/$ZnCl_2$ precipitation, essentially removes the bottleneck (multiple column cycles, large buffer requirements, long processing times) that occurs when the traditional Protein A process is matched with a high-titer harvest.

The process developed here utilizes one clarification step and three chromatographic purification steps in order to purify antibody precipitate. Product in its precipitated state is first re-solubilized, and then sent through two depth filters (C0HC and X0HC) in sequence in order to decrease turbidity by removing insoluble species. Depth filtration is followed by anion exchange chromatography in flow-through mode, cation exchange chromatography in bind/elute mode, and mixed-mode anion

exchange/hydrophobic interaction chromatography in flow-through mode. The development and optimization of each of these clarification and purification operations constitutes the focus of this thesis. A reversed-phase HPLC assay was also developed in order to verify the process is able to remove any residual PEG left over from precipitation. The end result is a process surrounding PEG/$ZnCl_2$ precipitation that can purify antibody product to within acceptable regulatory limits for host cell protein, DNA, and high molecular weight product aggregates. Overall process yield and impurity reduction are comparable to what is offered by traditional Protein A-based processes. Precipitation is a very useful technology because of its ability to decouple upstream and downstream processing while taking full advantage of the increase in productivity from high-titer cell culture processes. The optimized process developed here has proven it is capable of purifying precipitated antibody product to within acceptable impurity levels, highlighting its capability as a next-generation alternative to Protein A-based processes.

Designing a Next-Generation Antibody Purification Process by Integrating a Decoupling Precipitation Capture Step

by
Akshay Nitish Nadkarni

A thesis submitted to the Graduate Faculty of
North Carolina State University
in partial fulfillment of the
requirements for the degree of
Master of Science

Biomanufacturing

Raleigh, North Carolina

2014

APPROVED BY:

_____	_____
Dr. Gary Gilleskie Chair of Advisory Committee	Dr. Ruben Carbonell
_____	
Dr. Baley Reeves	

BIOGRAPHY

Akshay Nitish Nadkarni was born in Mumbai, India, and moved with his family to the United States in 1992. After settling in Cary, NC in 2004, he attended Green Hope High School, where he graduated with honors in 2008. The author successfully completed his Bachelor of Science in Biomedical Engineering at Duke University in 2012. During his time as an undergraduate, he was awarded the Pratt School of Engineering Undergraduate Research Fellowship. In collaboration with Dr. David Needham, the author further developed a novel method of protein dehydration called “microglassification”, introducing him to the fields of molecular biology and purification of therapeutic proteins.

Akshay enrolled in the Master of Science in Biomanufacturing program at North Carolina State University following his undergraduate career. Through this program, he obtained valuable knowledge and technical skills in both upstream and downstream process development for the manufacture of biologics. He further applied these skills in collaboration with Biogen Idec, conducting the research which ultimately forms the basis of this thesis project.

ACKNOWLEDGMENTS

Working in collaboration with NCSU and Biogen Idec on this project was an amazing opportunity, and I would like to express my gratitude to all the people who helped me along the way. I would like to thank Dr. Sanchayita Ghose, Dr. Yinying Tao, Dr. Lynn Conley, and the rest of the Process Biochemistry – Small Scale Purification group at Biogen Idec for generously providing their knowledge, guidance, and experience during this project. I want to express my sincere appreciation for the advice and insight provided by my advisory committee members, Dr. Ruben Carbonell, Dr. Gary Gilleskie, and Dr. Baley Reeves. I am also very thankful to Dr. Michael Flickinger and Christopher Smith, from the BIOM program at NCSU, for helping to make this project a possibility. Finally, I would like to thank my family and friends for their constant support, love, and encouragement – without them this achievement would not have been possible.

TABLE OF CONTENTS

LIST OF TABLES

LIST OF FIGURES

CHAPTER 1 - INTRODUCTION

The work presented in this thesis aims to design a next-generation antibody purification process that integrates a protein precipitation technology for decoupling upstream and downstream processing.

Recent research efforts and technological breakthroughs in mammalian cell culture technology have led to increased productivity in upstream processes for monoclonal antibody production. Many antibody processes utilizing CHO cells as a host organism for expression are taking advantage of intrinsic characteristics of the cell line, such as high expression levels and ability to grow in chemically-defined media, in order to achieve high product titers [1]. Within the biotechnology and pharmaceutical industries, several CHO-based antibody production processes in the development pipeline have already reached the long-standing target of 5 grams of antibody per liter of upstream cell culture harvest [2]. The focus for upstream processing has now shifted to producing a 10 gram per liter process, something that is expected to be achieved in the near future. Current mAb purification processes that were designed to accommodate incoming titers of 5 grams per liter will eventually be faced with significant bottlenecks associated with this increase in incoming product concentration [3], [4]. In order to take full advantage of the productivity gains presented by the increase in incoming product titer, a higher throughput and more cost effective downstream purification process must be designed.

A mAb purification platform with protein precipitation as a decoupling step can provide the significant cost and efficiency advantages that are desired, not to mention additional logistic advantages that are gained due to the unique nature of protein precipitation. The next-generation monoclonal antibody purification process that is the focus of this thesis

integrates a protein precipitation technology that revolves around the synergistic effect gained by combining the precipitation mechanisms of polyethylene glycol (PEG) and zinc chloride. The precipitated antibody product can be frozen and stored for later processing or shipped to alternative locations for further processing, effectively 'decoupling' upstream and downstream processing for antibody products. This gives additional flexibility in processing options that is not available with current, traditional Protein A-based processes, making protein precipitation via PEG and zinc chloride a very attractive and advantageous innovation. The work detailed in this paper describes the utilization of this novel precipitation technology, and the development of a next-generation downstream process tailored for purification of the precipitated antibody product.

CHAPTER 2 – BACKGROUND INFORMATION

2.1 – Purification of Antibodies

Traditional downstream processing platforms for monoclonal antibody therapies typically use Protein A (ProA) affinity resin chromatography as the primary product capture step due to the high physiochemical selectivity exhibited by the ligand [5]. A Protein A capture step is normally run in bind/elute mode, where mAb product present in the incoming upstream harvest is sent through the stationary resin and allowed to bind to the Protein A ligand with very high affinity. Binding of product in this stage can also be enhanced using high concentrations of kosmotropic salts, glycine, and/or lowered temperatures [5]. Once bound to the column, antibody product elution is achieved by lowering the pH of the mobile phase. This increases the electrostatic repulsion force between the ligand and the antibody while decreasing the hydrophobic contact area between the two, and results in antibody product coming unbound from the resin. The product is subsequently collected in the elution pool and sent to further polishing chromatography steps.

Applying Protein A affinity as a capture step for processes with large harvest volumes and incoming titers of 10 g/L or greater can result in significant bottlenecks. Typically, Protein A resins have binding capacities of 20 to 50 grams of antibody product per liter of resin. Due to this restriction either existing columns must be cycled numerous times to capture incoming material, or larger columns must be packed at considerable additional expense. The expense of Protein A resin (> $10,000/liter) is prohibitive to this measure, and is the reason for an overall desire to minimize the size of the column used or eliminate the Protein A step altogether. Increasing the number of cycles in order to handle the bump in incoming

product also involves increased buffer volume requirements, tank capacities, and filtration areas. Theoretical solutions to this bottleneck problem have been identified, and involve the use of “very large scale” Protein A processes which utilize “greenfield” facility designs and 1,500 liter Protein A columns [6]. However, this size of Protein A column would cost between $15 million and $20 million, which is a significant capital investment. Additionally, while “greenfield” facilities are ideal for this type of solution, they also come with cost and logistic hurdles. It is highly impractical to implement a “very large scale” Protein A process in an existing facility without making significant alterations to the facility footprint. These limitations of Protein A resins, as well as the unfeasibility of adapting traditional Protein A processes, have led to the pursuit of more productive, cost efficient alternatives for antibody capture.

The advent of low-cost cation exchange resins that have high binding capacities (between 40 and 100 g/L) and can handle relatively high flow rates has resulted in multiple investigative processes utilizing cation exchange chromatography as a product capture step [7]. Arunakumari et al. describe a process where a high-capacity CEX resin was used to capture concentrated antibody product from harvest at purity > 92% and yield > 82%, lending weight to the argument that CEX resins can effectively be used in place of Protein A [8]. Two other frequently reported antibody capture methods involve the use of hydrophobic charge induction chromatography (HCIC) resins and synthetic Protein A resins. Antibody binding to HCIC resins occurs due to a combination of hydrophobic and ionic interactions between the antibody product and the resin. Product will bind to HCIC ligands without the high salt concentrations required for traditional hydrophobic interaction chromatography, and can be disassociated from the resin without using the low pH elution typical of Protein A steps. Synthetic ligands have also been developed that mimic the hydrophobic binding domains of Protein A resins, but can be produced in non-recombinant

processes that involve techniques such as protein engineering, phage display, and synthetic chemistry [9]. Types of synthetic ligands include triazine ligands and peptide ligands of varying lengths. A recent review article that discusses the advent of small synthetic molecules and peptides as affinity ligands brings to light the fact that these new synthetic ligands and associated resin scaffolding can match the purification performance and recovery typically associated with Protein A affinity chromatography [10].

Non-chromatographic alternatives to Protein A capture have also been investigated. Aqueous two-phase processing systems (ATPS), methods in which product segregates to an aqueous phase containing polymer (such as PEG) over a separate aqueous phase containing salt, have proved an effective platform for the integration of clarification, concentration, and purification of antibody product in one single step [11]. While a PEG-citrate ATPS has been shown to capture IgG product at a yield of 99% and a purity of 96%, application of ATPS systems at production scale are difficult because the partitioning mechanism that yields the two distinct phases is poorly understood [12], [13]. Traditional precipitation techniques using high concentrations of salts, along with techniques such as metal ion affinity and polymer-induced steric exclusion, are being modified to improve efficiency and selectivity [14]. A novel method of antibody precipitation using controlled addition of polyelectrolytes such as polyvinylsulfonic acid and polystyrenesulfonic acid to pH-treated cell culture harvest pools has shown promise as both a capture step and a purification step [15].

Following the capture step, the remainder of the standard process for antibody purification consists of two to three unit operations in succession. The Protein A eluate is next held at low-pH conditions for viral inactivation, neutralized, then typically run through an anion exchange resin in flow-through (FT) mode. Low-pH conditions (between pH 3 to 4) are

known to irreversibly damage virus particles by destroying their lipid layers and protein coats. Ion exchange resins are used as polishing steps because of their ability to bring the product to acceptable purity levels, removing residual host cell proteins (HCP), endotoxins, nucleotides, virus particles, and leached Protein A particles, among others. When running anion exchange (AEX) in flow-through mode, buffer conditions (mainly pH) are set such that the antibody passes through the positively charged resin while strongly electronegative contaminants are captured. In AEX flow-through mode, significant reductions in DNA, retrovirus, and endotoxin levels are seen but the ability to reduce leached Protein A and host cell protein is compromised [3]. Cation exchange chromatography can also be used as a polishing step here, however these are typically run in bind/elute (B/E) mode where antibody product binds to the resin while other impurities such as host cell proteins, DNA, and some product aggregates flow through [16].

The next step incorporated into the downstream purification platform is hydrophobic interaction chromatography (HIC) in flow-through mode. By choosing buffer conditions carefully, the slightly hydrophobic product of interest is allowed to flow through the stationary resin while impurities with higher hydrophobicity than the antibody product (such as misfolded proteins, HCP, aggregates, dimers, trimers, tetramers, and leached chromatographic ligands) bind to the similarly hydrophobic resin. These impurities are consequently removed from the flow-through pool containing the antibody product, making HIC a very powerful purification step.

Depth filtration steps are sometimes included in the downstream process whenever clarification of the product stream is required. Conventionally, depth filtration is used for the primary purpose of fine particulate removal, but research suggests that the adsorptive properties of depth filters can be exploited to effectively remove soluble species as well

(depending on the selection of buffer conditions) [17]. Depth filtration can be included before the Protein A step to clarify cell culture harvest, and is sometimes used to clarify Protein A eluate if formation of particulates due to impurity precipitation occurs at low-pH conditions. After the purification steps, mAb downstream purification platforms typically include a filtration step designed to remove any residual virus particles, followed by an ultrafiltration and diafiltration (UF/DF) step to concentrate the product and buffer-exchange it into the final formulation buffer [18].

2.2 – PEG/$ZnCl_2$ Precipitation

As mentioned before, multiple drawbacks to using the traditional Protein A capture step for high titer mAb products have prompted the development of protein precipitation technology as a high-throughput, cost-effective decoupling step. The precipitation technology utilized here offers considerable efficiency and productivity gains as a result of synergy between separate PEG and zinc chloride precipitation mechanisms. To fully understand how this precipitation functions, it is important to know how both PEG and zinc chloride precipitation function separately. The mechanism of action of zinc chloride precipitation follows the typical framework of metal ion affinity precipitation; protein aggregation is induced by the addition of free metal ions, which cause reactive precipitation of protein monomers via cross linking [19]. Zinc is commonly used for protein precipitation at process scale, and has been utilized for the capture of human plasma proteins, among other biologics.

The presence of antibody product alongside free zinc ions (in solution after disassociation of zinc chloride salt) causes the ions to coordinate with surface-exposed histidine residues on the antibody molecules. This in turn causes the formation of metal-protein complexes,

which cross-link with remaining unbound sites on other antibody molecules, thus facilitating protein aggregation. This process continues until the antibody aggregates are no longer able to remain in solution, resulting in precipitation of the antibody product. Mathematical models of metal ion affinity precipitation show that increasing the number of ion binding sites on the target protein surface increases the rate of aggregation and precipitation, a claim which is reinforced when considering the smaller aggregation time constants associated with the precipitation of immunoglobulins versus albumin molecules (which have fewer Histidine residues than immunoglobulins) [20].

Antibody precipitation is started by the addition of zinc chloride to concentrated harvest and then driven further by the addition of a PEG/Imidazole solution. Protein precipitation via addition of PEG occurs because of preferential exclusion of PEG from protein surfaces, due to the steric exclusion of hydrated PEG molecules [21]. PEG by nature is a non-ionic, polar molecule and as such is soluble in a polar solvent such as water. When put into solution alongside high concentrations of protein, PEG has strongly repulsive interactions with the protein. These interactions become stronger with an increase in PEG size and/or concentration [22]. In order to relieve these thermodynamically unfavorable repulsive interactions, inter-protein aggregate complexes are formed between protein molecules in solution. Eventually, protein aggregates accumulate to the point where they can no longer remain in solution and subsequently precipitate out. The figure below shows the effect of using low-molecular weight PEG as a sole antibody precipitation agent. It is apparent that increasing PEG concentration leads to greater preferential exclusion between PEG and protein, and therefore greater precipitation yield and purity. Also, precipitation efficiency is higher at lower temperatures (4^0 C versus 25^0 C).

Figure 2.1, below, illustrates the main steps involved in this PEG/$ZnCl_2$ protein precipitation operation. Concentrated harvest (via ultrafiltration/diafiltration of native harvested CHO cell culture fluid) is combined with zinc chloride solution and polyethylene glycol/Imidazole solution at controlled rates. This results in the formation of a thick 'paste' containing precipitated antibody material. This paste is then centrifuged and solidified into a pellet, yielding highly - concentrated antibody product which can be stored at -20 ^{O}C to -70 ^{O}C. Studies have shown that the product in this form can remain viable for a period of 12 months or longer, meaning that the product can be stored for purification at a later date or shipped to a different site for purification elsewhere, effectively 'decoupling' upstream and downstream processing. Once ready to be further purified, the product is re-solubilized in a set volume of 100 mM Histidine solution and run through the rest of downstream process. United States patent application number 12/425,328, awarded to collaborators at Biogen Idec, explains this method of protein precipitation in greater detail [23].

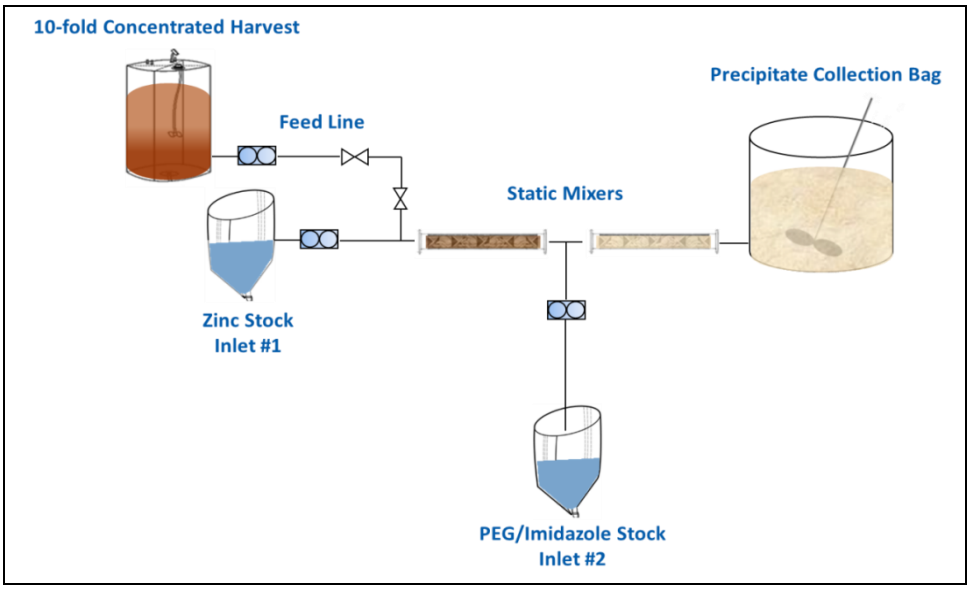

Figure 2.1: Precipitation using PEG and $ZnCl_2$ through static mixers. The concentrated HCCF is fed in-line through A static mixer, where it is blended with a $ZnCl_2$ stock solution. The resulting blend is fed through a second static mixer, where it is mixed with a PEG and Imidazole stock solution.

As mentioned before, the effectiveness of the PEG/$ZnCl_2$ precipitation is due to the synergy gained by combining the effects of (first) zinc chloride metal affinity precipitation and (second) PEG precipitation. Synergy, here, is defined as any additional yield gained over and above the additive effects of each individual precipitation mechanism. The addition of zinc chloride to the concentrated harvest allows for cross-linking and primary antibody aggregate particle formation. When the PEG/Imidazole solution is added, the PEG is thought to drive further aggregation of the already-formed primary aggregates, resulting in macroparticles of protein that precipitate out of solution. The added Imidazole serves to compete for non-specific metal ion binding sites, ensuring that the zinc only finds surface-exposed Histidine residues on antibody molecules. Previous development studies have shown that greater than 90% antibody precipitation yield is typically achieved when

combining these two precipitation mechanisms in the fashion described above, and that the gain in yield due to the synergistic precipitation versus each individual mechanism can be as high as 131%.

There are multiple advantages to capturing and storing antibody product via PEG/$ZnCl_2$ precipitation. The ability to 'decouple' upstream and downstream processing by inserting a precipitation step in between is gained because of the fact that precipitates are stable for greater than 12 months at -70 ^{O}C. An entire high-titer harvest can be captured and processed in smaller, 'decoupled' sub-batches over the course of the storage lifetime of the batch. A stability study conducted on a specific mAb product which was precipitated, captured using centrifugation, and stored at 2-8 ^{O}C, -20 ^{O}C, and -70 ^{O}C showed that storage at either -70 ^{O}C or -20 ^{O}C for at least 12 months is feasible and does not result in aggregation or significant molecule-to-molecule differences that would compromise the safety or efficacy of the product. The percentages of high molecular weight (HMW) aggregates, low molecular weight fractions, and dimers from material stored at -70 ^{O}C for 13 months and then resolubilized are similar to corresponding values for material that has just been captured, meaning that storage at -70 ^{O}C is a viable option for product in this precipitated form.

The ability to decouple upstream and downstream processing by holding product as a precipitated intermediate will also provide flexibility in planning manufacturing operations. Consecutive high-titer upstream campaigns can be run to meet the level of product demand, and material produced can be precipitated and stored for further processing only when needed. Once the product has been precipitated, it can be shipped to any facility in the world in order to directly supply local markets.

CHAPTER 3 - OBJECTIVE

The aim of this project is to integrate protein precipitation technology as a primary decoupling step in a new, next-generation downstream process for antibody purification. Although precipitation is attractive as an alternative to traditional Protein A capture because of its reduced cost, decoupling advantages, and ability to handle high product capacities, studies suggest that the impurity clearance capability of precipitation itself is relatively poor in comparison. If precipitation is to function as a capture step in a process that is as robust and effective as a Protein A-based process, then the burden of impurity clearance must fall on the purification steps that follow protein precipitation. Table 1.1 shows final product impurity limits recommended by the Food and Drug Administration (FDA) and other industry standards that the purification process must meet or exceed [24 – 28]. A re-design of the traditional monoclonal antibody purification sequence is required in order to meet these specifications. The bulk of the experimentation described here has been done to develop this new purification process.

Table 1.1: Final product impurity profile.

Impurity	Industry Specification	Source for Specification
Host Cell Protein	< 100 ppm	FDA recommendation
DNA	< 100 pg/dose	FDA recommendation
HMW %	< 1.00%	Product-specific standard
Free PEG	< 2.5 ug/mL	Industry standard

Initially, it has been suggested that a three-column purification process should be evaluated with protein precipitation as the primary decoupling step. Re-solubilized product will be

sent through a depth filtration skid in order to remove fine particulates and some soluble species from solution. Following depth filtration, product will be purified using anion exchange chromatography in flow-through mode in order to remove acidic contaminants such as HCPs, DNA, and virus particles [29]. There is some freedom available in selecting which AEX technology will be used for purification, and two widely used methods will be evaluated. These include traditional AEX chromatography resins and fast-flow anion exchange membranes. Effective use of AEX chromatography requires the use of stringent pH and/or conductivity ranges to achieve sufficient resolution, which often means that the load sample must be manipulated in a very complex manner. Membrane technology offers the logistical advantage of being much faster and more productive than traditional column-based chromatography methods [30].

Cation exchange chromatography (CEX) in bind/elute mode will be evaluated as the second column step in the purification process. Newer generations of CEX resins have become available which provide a level of binding capacity (> 100 g/L) that allows CEX in bind/elute mode to be commercially viable. CEX is a valuable tool for residual HCP removal as well as Protein A leachate removal [31]. Finally, a third column will be applied in the process to serve the purpose of aggregate removal. A mixed-mode AEX/HIC resin will be evaluated to achieve this specific purification. Applying mixed-mode chromatography methods can present different purification powers for different types of impurities, and combining HIC with AEX purification can potentially provide significant aggregate removal in addition to the expected HCP clearance seen when using AEX alone. Table 1.2, below, compares the new proposed process with the traditional process for mAb production.

Introduction of reagents during the PEG/$ZnCl_2$ precipitation step comes with the mandate that these reagents be somehow removed by the subsequent purification sequence. There

are multiple ways to remove PEG and zinc chloride from the product stream. Washing the precipitation pellets after centrifugation will eliminate any residual PEG or zinc chloride that may be left on the surface of the solid pellet. Including a cation exchange chromatography step in bind/elute mode will also remove free PEG from the product stream, as it is unable to bind to the charged resin in the same manner as antibody product. Selection of a 30 kilodalton (kDa) molecular weight cutoff for the final UF/DF operation, which concentrates and buffer-exchanges the final process material, allows PEG and zinc chloride to flow through the filter membrane while product is retained. To verify that PEG will be removed by the process even prior to the final UF/DF step, a reversed-phase HPLC assay utilizing Corona charged aerosol detection will be developed that will determine the amount of residual PEG in the final process sample. Since any free zinc chloride remaining in the final process sample can be considered as simply another low-molecular weight salt component in the buffer, it is assumed that free zinc will be cleared by the final UF/DF operation.

Table 1.2: Traditional and proposed new purification processes for mAb production.

Step	Traditional Process	Proposed Process
Capture/Decoupling	Protein A (bind/elute)	PEG/$ZnCl_2$ Precipitation
Clarification	Depth filtration	Depth filtration
1st purification step	AEX (FT)	AEX (FT) or AEX fast-flow membrane (FT)
2nd purification step	HIC (FT)	CEX (bind/elute)
3rd purification step	N/A	HIC (FT) or mixed-mode AEX/HIC (FT)

The goal of this research endeavor is to develop a new monoclonal antibody purification process with protein precipitation as the primary decoupling step. Such a process is highly desirable because it can potentially take advantage of the increase in productivity from

high-titer cell culture processes, and will be seen as a high throughput and cost-effective alternative to traditional Protein A-based purification processes. The ability of protein precipitation to 'decouple' upstream and downstream processing will provide manufacturing flexibility and options for future processing of stored product, advantages that will satisfy multiple logistic business drivers. Work will be done to develop and optimize a process for 'Antibody A' purification, consisting of precipitation plus three chromatographic purification steps. In order to show the feasibility of this process, it will be demonstrated that the process will purify antibody product to the extent where final target impurity levels (HCP, DNA, HMW aggregate) are within acceptable standards. This will prove that the new process is robust enough to be applied in a commercial setting, validating the process's feasibility as a next-generation approach to antibody purification.

CHAPTER 4 – PEG/$ZnCl_2$ PRECIPITATION AND RE-SOLUBILIZATION

4.1 – Materials and Methods

Harvest cell culture fluid (HCCF) containing approximately 5 g/L of 'Antibody A' (mAb A, ~150 kDa, isoelectric point ~ 6.5) from a CHO cell upstream process was concentrated 10x through a 30 kilodalton (kDa) ultrafiltration membrane on a lab-scale tangential flow filtration system (both from Novasep, Boothwyn PA, USA). The concentrated material was diafiltered with equilibration buffer (35 mM BisTris, pH 6.5, 2.0 mS/cm) until reaching the expected buffer conditions (pH 6.5, 2.0 mS/cm). Both ultrafiltration and diafiltration steps were performed at ambient temperature.

Figure 2.1 shows the equipment and setup used for precipitation. The precipitation skid consists of three peristaltic pumps (Cole-Parmer, Vernon Hills IL, USA) which deliver process intermediate and precipitation reagents. Static in-line mixers (Cole-Parmer), 3/16" in diameter, were fitted into 1/4" tubing (Cole-Parmer) to provide sufficient mixing of product with reagents. The zinc chloride mixer length was cut to 1.18 inches, while the PEG mixer length was cut to 4.75 inches. The skid was flushed with water and then flushed with equilibrium buffer before product loading began. Product was fed through the entire system at a controlled flow rate. Zinc chloride solution was then fed through the first static mixer and allowed to mix with the product feed. Following this, PEG/Imidazole solution was released through the second static mixer and allowed to mix with the product stream. Equilibrium buffer and precipitation reagent solution compositions are kept proprietary, and flow rate, mixer diameters, and mixer lengths were specifically set in order to provide adequate time and surface area for each reagent to sufficiently mix with the product stream. Upon complete mixing with both reagents, retention of the product stream began.

Once precipitation was completed, the collected precipitate was split into aliquots and centrifuged at 5000 rpm for 5 minutes at 4 ^{0}C. Supernatant was decanted and discarded, while precipitation pellets were stored at -70 ^{0}C until required.

To recover precipitated material, precipitate pellets were thawed at 4 ^{0}C overnight. 100 mM Histidine solution (pH 7.5) was then added to each pellet tube as a re-solubilizing agent at a pellet-to-Histidine-solution volume ratio of approximately 1:1. Tubes containing pellet and Histidine solution were allowed to mix on shaker tables for 24 to 36 hours at 4 ^{0}C, until pellets had completely dissolved into solution. Titer values of the precipitate re-solubilization pool were measured using ProG-HPLC.

4.2 – Results and Discussion

In order to generate precipitated antibody material for process development work, a large batch-scale PEG/$ZnCl_2$ precipitation was conducted using the precipitation methods described in Section 4.1. Approximately 4.5 liters of 10x concentrated mAb A cell culture harvest were input to the precipitation skid. Upon conclusion of mixing with zinc chloride and PEG, the resulting precipitate mix was split into multiple 50 mL tubes and 500 mL bullet tubes for centrifugation. All of these aliquots were centrifuged and decanted, and the resulting mAb A precipitate pellets were frozen at -70 ^{0}C until needed. This frozen bank of mAb A material served as the product reservoir for all process development work. Average yield of precipitation was greater than 99%, based on a mass balance of recovered product after re-solubilization with 100mM Histidine.

CHAPTER 5 – OPTIMIZATION OF CLARIFICATION STEP

5.1 – Methods and Materials

In preparation for the "Pmax" experiment, a large pool of re-solubilized mAb A precipitate was generated, then diluted to 25 mg/mL in low salt buffer (30 mM BisTris, pH 6.5, 2.0 mS/cm). X0HC and C0HC filters (EMD Millipore, Billerica MA, USA) with areas of 23 cm^2 were flushed with water and low salt buffer. Loading of both filters with mAb A product was done simultaneously. Filters were loaded at a flux of 100 liters per square meter of filter area per hour (LMH). A FilterTec instrument (Scilog, Madison WI, USA) was utilized to monitor pressure as a function of time and loading. Turbidity values were taken periodically of each filtrate pool. Loading on filters was halted when pressure exceeded 20 psi or when filtrate pool turbidity exceeded 50% of load turbidity. After loading, both filters were flushed with 35mL of low salt buffer. These flush volumes were added to their respective filtrate pools. Titer values of each pool were measured using ProG-HPLC in order to determine yield. A residual HCP assay was also conducted on each filtrate pool.

To model HCP breakthrough on an X0HC filter, a second 23 cm^2 filter was conditioned and loaded to approximately 1700 g/m^2 with re-solubilized mAb A precipitate diluted in low salt buffer. Fractions were collected corresponding various levels of mAb A loading onto the filter. A 50mL filter flush with low salt buffer was collected in a separate fraction. All fractions were analyzed for HCP content and yield using residual HCP and ProG-HPLC assays.

In order to determine the filtration sequence for the final process, a 23 cm^2 C0HC filter was conditioned and loaded to approximately 1700 g/m^2. Upon conclusion of loading, the filter was flushed with 115mL of low salt buffer. Fractions were taken at various levels of flush

volume corresponding to multiples of filter membrane dead volume (MV). These were analyzed for titer by ProG-HPLC to determine amount of mAb A present. The final filtrate pool, consisting of filtrate plus the first 60mL of flush, was sent through a 23 cm^2 X0HC filter until the filter was loaded to 532 g/m^2. Flush fractions were collected in a similar manner to the C0HC filtration and analyzed for titer. The final series filtration pool consisted of X0HC filtrate plus the first 100mL of flush volume. All samples (C0HC load, C0HC filtrate, X0HC filtrate) were analyzed for titer and HCP content.

5.2 – Results and Discussion

5.2.1 – Low pH Adjustment of Re-solubilized mAb A Precipitate

Low pH adjustment is a frequently utilized way to clarify cell culture harvest material in order to remove soluble impurities such as HCP's and DNA. The typical method involves lowering the pH of the harvest material to the point where species other than the target product undergo isoelectric precipitation. The majority of CHO host cell proteins have isoelectric points (pI) in the range 4.0 to 7.0 [32]. As the pH is lowered to near the HCP pI, the lack of overall-net-charge on these proteins causes them to associate and precipitate out of solution. At such low pH's, the typically basic isoelectric points of antibody products protect them from flocculation. Reduction of up to 20% of CHO host cell proteins has been reported by adjusting the pH of harvest material to 4.0 [33]. In a separate study, a 3-log DNA level reduction was achieved by adjusting cell culture harvest down to pH 4.7 [34].

When readying product for experimentation, it was noticed that re-solubilized mAb A precipitate that had been diluted in low salt buffer (pH 6.5, 2.0 mS/cm) was too turbid to be 0.22 micron filtered or loaded onto a column. In order to remedy this issue, the sample was adjusted to pH 5.5 (the midpoint of the optimal 4.0 to 7.0 range), centrifuged to remove

precipitated species, and then adjusted back to the desired load pH. While this reduced the turbidity of the load samples to the point where they could be filtered, this process resulted in a significant amount of product loss. This was thought to be due to co-precipitation of product with impurities that become insoluble at low pH values.

To identify the root cause for the product co-precipitation, several factors were investigated. Re-solubilized precipitate was compared with native mAb A HCCF and 10x concentrated mAb A harvest to see if any potential structural modifications during PEG/$ZnCl_2$ precipitation lead to antibody product being more prone to co-precipitation during low pH adjustment. High titer (10x concentrated) harvest was chosen to see if mAb concentration plays an effect in co-precipitation. Secondly, re-solubilized precipitate material was diluted in both low and high ionic strength buffer to see if high salt improves product retention during low pH adjustment. Evidence suggests that the presence of cations during low pH adjustment shields electrostatic interactions between the target product and flocculated components.

Re-solubilized mAb A precipitate was diluted in low salt buffer (30mM BisTris, pH 6.5, 2.0 mS/cm) to a concentration of 7 g/L. A second sample of re-solubilized mAb A precipitate was diluted to 7 g/L in high salt buffer (75mM sodium phosphate, 35mM NaCl, pH 7.31, 12.41 mS/cm). A third sample of 10x concentrated mAb A harvest (via single pass tangential flow filtration) was obtained. All three samples were adjusted to pH 5.5 via the addition of 25% acetic acid, then centrifuged at 5000 rpm for 5 minutes. Supernatants were harvested and adjusted back to original pH values via the addition of 0.9 M BisTris, 0.24 M Tris solution. Titer values were obtained by Protein G-HPLC assay (discussed further in Section 6.1.4) before and after low pH adjustment to calculate product retention.

Figure 5.1 below shows the change in appearance of the mAb A HCCF during the low pH adjustment process. It should be noted that native mAb A HCCF has no issues being passed through a 0.22 micron filter. Figure 5.2, for comparison, shows the same low pH adjustment process for re-solubilized mAb A precipitate diluted in low salt buffer. There is marked increase in turbidity after re-solubilized mAb A precipitate is adjusted to pH 5.5, and a significant reduction in turbidity between that sample and the post-centrifugation supernatant.

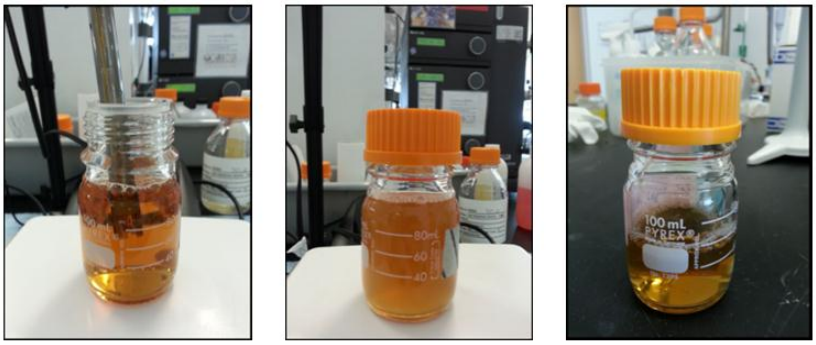

Figure 5.1: Low pH adjustment of mAb A HCCF. Left: Native mAb A HCCF. Center: HCCF adjusted to pH 5.5. Right: Post-centrifugation supernatant.

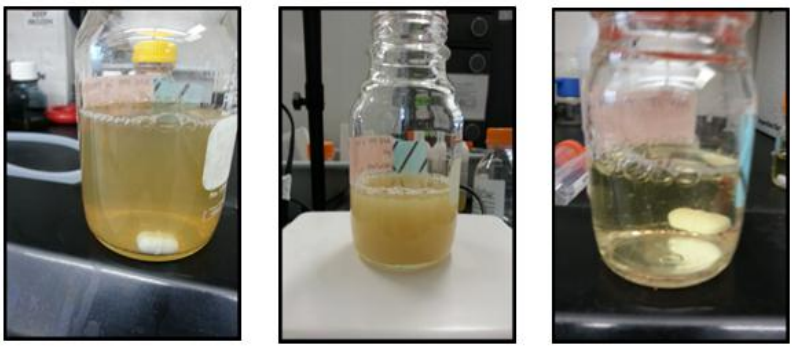

Figure 5.2: Low pH adjustment of re-solubilized mAb precipitate diluted in low salt buffer. Left: Pre-pH adjustment. Center: adjusted to pH 5.5. Right: Post-centrifugation supernatant.

Table 5.1 below shows results of yield calculations for the low pH adjustment operation for each of the four samples: native HCCF, re-solubilized precipitate in low and high salt buffer, and 10x concentrated HCCF.

Table 5.1: Low pH adjustment yields. Yields calculated by dividing the mass of mAb A present in the final supernatant by the mass of mAb A present in the sample before pH adjustment occurs.

Sample Material	Conc. (g/L)	pH	Cond. (mS/cm)	Yield (%)
HCCF Pre-pH Adjust	6.22	7.28	12.45	---
HCCF Post-pH Adjust	5.91	6.50	12.52	95.2
High Salt Buffer Pre-pH Adjust	7.18	7.36	11.14	---
High Salt Buffer Post-pH Adjust	6.15	6.48	11.62	85.7
Low Salt Buffer Pre-pH Adjust	7.00	6.73	1.68	---
Low Salt Buffer Post-pH Adjust	5.51	6.49	3.71	78.8
10x Harvest Pre-pH Adjust	50.09	7.65	9.68	---
10x Harvest Post-pH Adjust	48.29	6.57	10.82	96.4

Native mAb A HCCF sees relatively little product loss when low pH adjusted. In contrast, both the re-solubilized precipitate samples in high and low salt see very large amounts of product loss, between 14% to 21%. Increase in salt content did not significantly improve product retention during pH adjustment. Similar to the native HCCF, 10x concentrated harvest sees very little product loss. This leads to the conclusion that only re-solubilized precipitate samples show product loss when low-pH adjusted. A hypothesis for this effect is that the presence of re-solubilized HCP recovered alongside product from PEG/$ZnCl_2$ precipitation, when forced to precipitate upon low pH adjustment, causes mAb product to co-precipitate out of solution. This phenomenon has been observed previously in

experiments where mAb has co-precipitated out of low-pH Protein A elution pools which contain higher-than-normal HCP levels [18].

Both native HCCF and 10x concentred harvest have not been through PEG/$ZnCl_2$ precipitation and, as such, do not see product loss when low pH adjusted. PEG/$ZnCl_2$ precipitation may alter the structure of the mAb molecule slightly, making it more prone to co-precipitation by exposing hydrophpbic groups, for example. The presence of excess Histidine may play a role in co-precipitation as well. For native HCCF conditions, cations in solution can potentially interact with exposed Histidine groups on the antibody product, protecting it against electrostatic interactions with any negatively-charged flocculated impurities. In the case of PEG/$ZnCl_2$ precipitated material, free cations may bind with excess Histidine present in solution (from the re-solubilization solution). Surface Histidines are left exposed on the antibody product, leaving it unprotected against co-precipitation. The low yields associated with low pH adjustment mean that this operation is not feasible to ready the re-solubilized mAb material for column processing, and alternative measures (such as depth filtration) must be explored.

5.2.2 – Depth Filtration Optimization

Depth filtration is commonly utilized in antibody manufacturing processes in order to remove macromolecular species such as cell debris and colloidal compounds from the process feed stream. Depth filters are advantageous due to their ability to handle large process volumes in relatively short time periods. Most depth filters are single-use, and as such are easy to set up at process scale and require low up-front capital investments [35]. In single-use manufacturing facilities where a disposable centrifuge is not availiable, depth filtration is the ideal alternative option for clarification of process intermediates.

Initial depth filtration screening was performed by comparing the clarification and purification capabilities of two different types of depth filters. X0HC and C0HC filters, both manufactured by EMD Millipore, were investigated. C0HC filters have a nominal pore size between 2 and 0.2 microns, making them appropriate for the removal of large particluates. X0HC filters have an average pore size of less than 0.1 microns, limiting their particulate clearance capabilities. However, X0HC filters carry overall positive surface charges which can potentially provide impurity removal by adsorbing soluble negatively charged species while allowing mAb product to flow through at the right operating conditions.

First, a “Pmax” experiment was conducted on both types of filters to determine the maximum amount of mass of mAb A that could be loaded per unit area of filtration membrane. Filter load solution was at pH 6.5, 2.0 mS/cm operating conditions. Loading on a filter was stopped when either the pressure across the filter exceeded 20 psi, or the turbidity value of the filtrate exceeded 50% of the turbidity of the load.

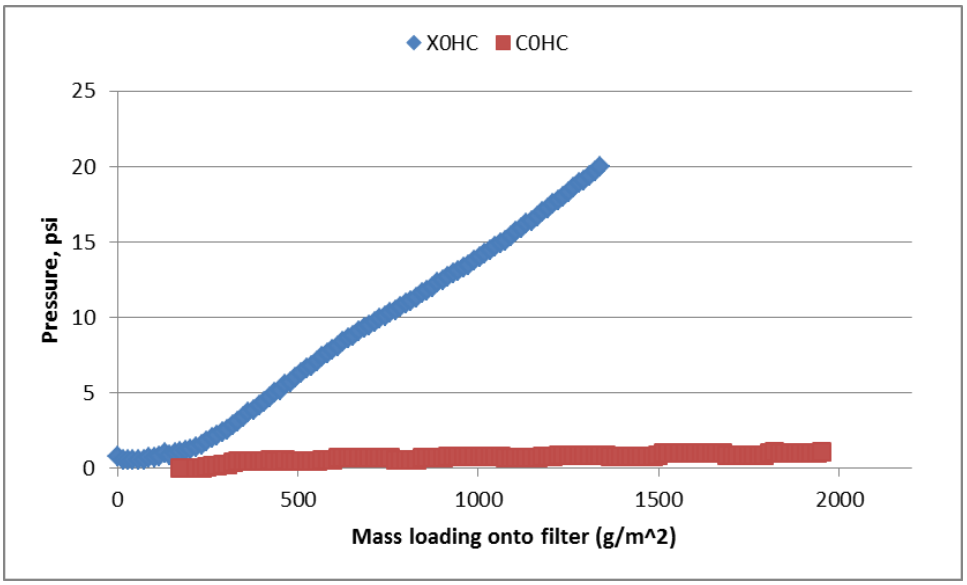

Figure 5.3: X0HC and C0HC Pmax filtration. Graph depicts pressure across the filters (psi) versus mass of sample loaded onto the filter membranes (g/m^2). Results for the X0HC filter are shown in blue, while results for the C0HC filter are shown in red.

Figure 5.3 shows pressure vs. mass of mAb A loaded onto each filter. The X0HC filter pressure (blue trace) increases linearly with filter loading and exceeds 20 psi after approximately 1350 g/m^2 of loading. Pressure across the C0HC filter (red trace) stays constant between 0 and 1 psi during the duration of sample loading. However, 50% turbidity breakthrough of the C0HC filtrate occurs at approximately 1950 g/m^2 of filter loading. The turbidity, HCP content, and product recovery for the collected filtration pools at maximum loading are summarized in Table 5.2. Yield values of both depth filtrations were within the desired range for such a depth filtration step (85% or greater). However, little to no HCP clearance was observed on either filter at their respective maximum loadings. This suggests that after some loading limit, host cell proteins begin to break through the filter and flow into the filtrate pool (although this does not necessarily directly translate into a proportional increase in turbidity).

Table 5.2: Summary of Pmax Data. Turbidity fraction is calculated by dividing the turbidity of the filtrate pool by the turbidity of the load solution.

Experiment	Mass Loading (g/m^2)	Turbidity Fraction	HCP in Load (ppm)	HCP in Filtrate Pool (ppm)	Yield (%)
X0HC	1338	0.57	88703	80775	89.1
C0HC	1953	0.37	88703	84512	94.0

As X0HC filtration is theoretically more effective for soluble HCP removal, the decision was made to focus on optimizing the loading density on this type of filter to achieve better HCP clearance. To find the HCP breakthrough loading point for X0HC depth filtration, an additional study was conducted where a filter was loaded to approximately 1800 g/m^2, slightly above the maximum loading limit determined during the Pmax study. Filtrate fractions were collected at different amounts of product loading. The filtrate flush volume was collected and analyzed in a separate fraction. All fractions were assayed for host cell protein content, turbidity, and product yield.

Figure 5.4 below shows the trends of HCP content and yield as a function of loading density. As expected, both yield and HCP increase with increased filter loading. The low yield across the loading range is partially attributed to the large hold-up volume of the filtration system relative to the total volume. The figure does not include product recovered in the flush volume after filtration load was completed. Actual yield is expected to be significantly higher if product recovered in the post-load flush fraction is included. By doing this, the overall yield of the filtration operation increases to 86.3%. Lower yield during filtration may be due to high turbidity in the feed stream. This causes plugging of the filter membrane with large-diameter particles that can block passage of the product through the filter. A significant jump in cumulative HCP content of the filtrate pool occurs at approximately 900

to 1100 grams of product per square meter of filter area, as the HCP rises from ~20k ppm to ~65k ppm.

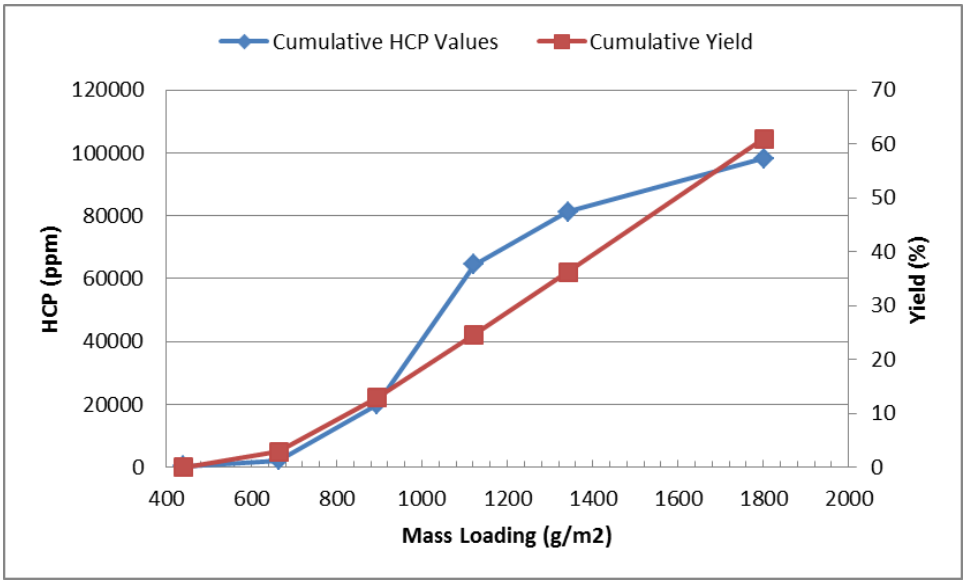

Figure 5.4: HCP and yield data for X0HC filtration fractionation. Cumulative HCP values (ppm) versus mass loading (g/m^2) are plotted in blue while cumulative yield values (%) versus mass loading are plotted in red.

Based on these results, it is estimated that a mass loading level of less than or equal to 900 g/m^2 is appropriate for the desired turbidity reduction and HCP removal. But, Figure 5.4 does not take into account the additional turbidity and HCP content that the filter flush volume will add when pooled with the filtrate. It is estimated that the actual mass loading required to obtain the desired turbidity and HCP reduction will be less than 900 g/m^2.

Given the limitations of the X0HC filter seen to this point, namely low HCP clearance, low yield, and high pressure, a revised filtration strategy is needed to serve as a more efficient and robust clarification step. To determine a filtration procedure that meets these criteria, a

sequence coupling C0HC and X0HC filtration together was investigated. The main cause of the rapid pressure increase on the X0HC filter was due to plugging of the filter membrane with particulates greater than the pore size of the membrane (> 0.1 um). To remove these particulates, the product feed can first be passed through a C0HC filter, which has a larger nominal pore size rating (2um to 0.2um) and will eliminate particulates that rapidly clog the X0HC membrane. As shown during the Pmax experiment, a C0HC filter can be loaded with relatively high product mass per unit membrane area without any pressure issues, while still retaining a high product yield.

Re-solubilized mAb A precipitate at pH 6.5, 2.0 mS/cm conditions was loaded onto the C0HC filter to approximately 1750 g/m^2. Optimization of flush volume collection was conducted to further improve product recovery. The C0HC filter was flushed with approximately 4.6 membrane volumes of low salt buffer following product loading. Fractions of the flush were collected and analyzed for product concentration to determine the amount of mAb A recovered. The C0HC filtrate was then directly loaded onto an X0HC filter to a level of 532 g/m^2. This X0HC filter was also flushed with 4.6 membrane volumes of low salt buffer to determine the additional amount of product recovered. Figure 5.5 below shows a plot of yield gained versus additional flush volume for both the C0HC filtration and subsequent X0HC filtration. Table 5.3 shows the results of the analytical testing done for this filtration sequence experiment.

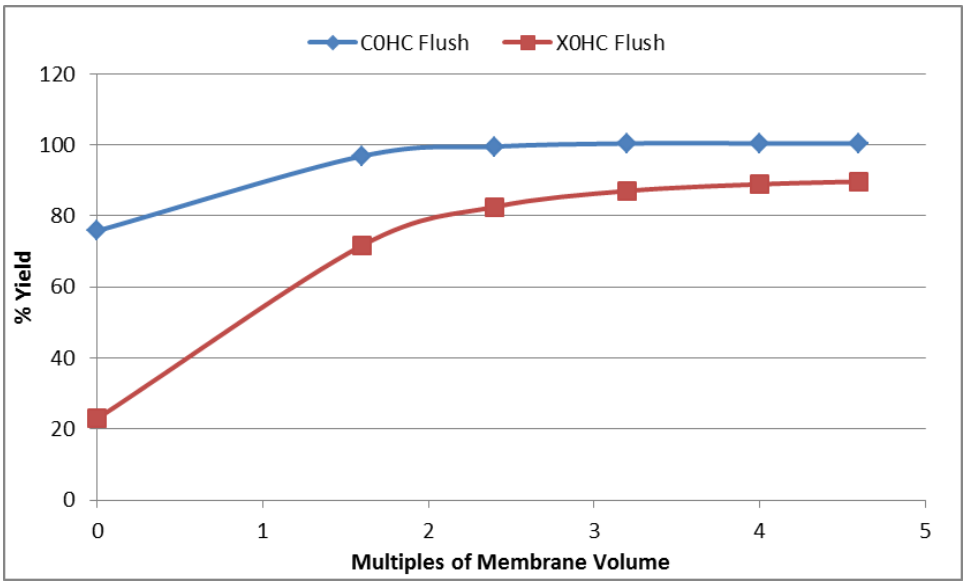

Figure 5.5: Yield gains from additional flush volume, C0HC and X0HC filtration. Graph depicts cumulative yield of mAb A recovered versus total flush volume in multiples of membrane hold-up volume (25mL). Results for X0HC filtration are shown in red and results for C0HC filtration are shown in blue

Table 5.3: Analytical results for C0HC – X0HC Depth Filtration. Summary of yield, turbidity, and HCP results for final specified filtrate pools.

Experiment	Mass Loading (g/m^2)	Turbidity Fraction	Max. Pressure (psi)	HCP in Load (ppm)	HCP in Filtrate Pool (ppm)	Yield (%)
C0HC	1748	0.53	0.68	100000*	80000*	97.2
X0HC	532	0.19	2.50	80000*	45941	86.9

* Data estimated from previous results

Figure 5.5 shows that increasing the flush volume of the filter following sample loading has a significant effect on step yield for the X0HC filtration. The C0HC trace has a high initial yield – this is a direct result of the high mass loading on the filter. Taking 2.4 membrane volumes (MV) of flush recovers an additional 20% of the product. In the case of the X0HC

filtration, this effect is more extreme. Since the filter was loaded with relatively little mass, initial product recovery in the flow-through pool alone is poor, only 23%. Taking 2.4 MV of flush and adding it to the filtrate pool brings the yield closer to 82%. If the flush volume is increased to 4 MV, another 4% to 5% of yield is gained. In addition to recovering product left in the hold-up volume of the depth filtration system, extra flush volume may help to release mAb product bound to the filtration membrane itself. Other experiments that investigated the use of various depth filters to recover mAb from cell culture harvest have reported that as much as 40 L/m^2 of flush volume is required to obtain a product recovery greater than 85% [36].

Table 5.3 shows the analytical results for the C0HC and X0HC filtrations in series. The overall yield of the C0HC and X0HC filtrations in sequence was 84.5%. Between the two filtrations overall, turbidity was reduced to 19.4% of the initial turbidity. The final filtrate pool was clear enough to be 0.22 micron filtered without any issues. Both filters in series brought the HCP content of the product stream down to below 50k ppm. Crucially, the inclusion of the C0HC filtration prior to the X0HC filtration resolved the pressure issues seen previously. With this depth filtration process, the maximum pressure seen by the X0HC filter was well within the recommended operational limits. Based on these results, this combination of C0HC and X0HC filtration with additional flush volume can be used to generate material with low turbidity and HCP content in a method that achieves high unit operation yield with no pressure issues. Therefore, the decision was made to integrate this C0HC – X0HC filtration sequence into the final process.

CHAPTER 6 – OPTIMIZATION OF PURIFICATION STEPS

6.1 – Methods and Materials

6.1.1 – AEX Condition Screening

A pool of re-solubilized mAb A precipitate was diluted to 10 g/L in low salt buffer (30 mM BisTris, pH 6.5, 2.0 mS/cm). An initial low pH adjustment was performed to decrease turbidity of this pool in preparation for chromatography operations. Following this, the product solution was titrated back to pH 6.5 using 0.9M BisTris, 0.24 M Tris adjustment solution.

A 0.66 cm diameter chromatography column (Omnifit, Danbury CT, USA) was packed with anion exchange (AEX) resin to a bed height of 11.7 cm in preparation for the AEX in flow-through step. The column was equilibrated with 5 CV's of low salt buffer, then loaded with mAb A sample to 200 grams of mAb A per liter of resin. Fractions were collected corresponding to 100 g/L loading and 200 g/L loading levels. Upon conclusion of the load phase, the column was washed with low salt buffer. This wash was collected in a separate fraction. The column was stripped with 1M NaCl buffer, and then sanitized with 3M NaCl, 0.5M NaOH buffer. All stages were run at a flow rate of 0.67 mL/min, corresponding to a 6 minute residence time on the column.

AEX fast-flow membrane chromatography was conducted using a 0.08 mL anion exchange membrane. The membrane was equilibrated with 50 mL of low salt buffer, then loaded to 5 grams of mAb A per mL of membrane volume. Fractions were collected at 2, 4, and 5 g/mL of loading. The membrane was washed with 50mL of low salt buffer, which was collected in a separate fraction. The membrane was then stripped with 1M NaCl buffer, re-equilibrated,

and discarded after use. All stages were run at a flow rate of 2.4 mL/min, corresponding to a residence time of 0.033 minutes. Flow rate was set according to manufacturer specifications. Fractions for both purification operations were analyzed for titer, aggregate levels, HCP, and DNA content using ProG-HPLC, SEC-HPLC, residual CHO HCP, and DNA Q-PCR assays, respectively.

6.1.2 – CEX Condition Screening

X0HC depth filtrate remaining from previous experiments was split up into three samples, each of which was adjusted to match one specific CEX load condition (pH 5.0, 5.0 mS/cm, pH 5.5, 5.0 mS/cm, pH 6.0, 5.0 mS/cm) via the addition of 25% acetic acid and 1M NaCl. A 0.66 cm diameter column to be used for all three CEX runs was packed to a bed height of 9.6 cm with CEX resin. Each run followed the same general procedure: the column was first equilibrated with 5 CV's of EQ buffer (50 mM sodium acetate) matching the pH and conductivity conditions for the specific run. This was followed by mAb A sample loading until the column reached 70 grams of mAb A per liter of resin. Loading limit was set based on previous optimization work for mAb A. The column was then washed with EQ buffer, before being eluted with 50 mM sodium acetate, 160 mM NaCl, pH 5.1, 18.77 mS/cm buffer. The column was then stripped with 1M NaCl and sanitized with 0.5 M NaOH before the next run was conducted. Flow rate was held constant at 0.56 mL/min (6 minute residence time). Titers and aggregate values at all stages were collected using ProG-HPLC and SEC-HPLC assays. Residual HCP and DNA assays were conducted on final CEX elution pools.

Native mAb A HCCF was sent directly through a 0.66 cm diameter column packed to a bed height of 19.5 cm with Protein A resin. The column was equilibrated with 5 CV's of 75 mM

sodium phosphate, 100 mM NaCl, pH 7.3 buffer. Following this, the column was loaded to 35 grams of mAb per liter of resin with mAb A HCCF. The column was washed with 3 CV's of EQ buffer, washed with 5 CV's of 50 mM BisTris, 1M NaCl, pH 7.0 buffer, and washed again with 5 CV's of 10 mM BisTris, pH 6.6 buffer. Elution of the mAb product was performed with 100 mM Glycine buffer (pH 3.0); collection began when the UV280 trace rose above 100mAU. Eluate was collected for 2.5 CV's. The column was subsequently sanitized with 4 CV's of 0.1 M NaOH. Flow rate was held constant at 1.11 mL/min (6 minute residence time). Final HCCF – ProA elution was adjusted to appropriate run conditions (pH 4.6, 12.5 mS/cm or pH 4.6, 5.0 mS/cm) via the addition of 2 M BisTris and 1 M NaCl. This material was run through a CEX column equilibrated at conditions matching the load in the same method described above.

Re-solubilized mAb A was sent through the C0HC – X0HC sequence and a larger-scale AEX in FT column in the manner described in Section 5.1.1 and Section 6.1.1. This AEX flow-through pool was then split into three samples; one was adjusted to pH 5.5, 5.0 mS/cm, another to pH 4.6, 12.5 mS/cm, and the third to pH 4.6, 5.0 mS/cm via the addition of 25% acetic acid and 1 M NaCl. All three samples were run on the same 0.66 cm by 9.6 cm CEX column and procedure used during previous CEX screening runs at equilibrium conditions matching respective load pHs and conductivities. Titer and HMW% values of all samples were taken using ProG-HPLC and SEC-HPLC assays.

6.1.3 – Mixed-Mode Condition Optimization

Multiple runs of mAb A depth filtrate over CEX were conducted to generate a pool of load material for mixed-mode optimization studies. DesignExpert software (Stat-Ease, Minneapolis MN, USA) was used to create a 2^3 factorial, 20-point experiment design which

varied pH, conductivity, and resin loading parameters. Samples of mAb A CEX eluate were adjusted to meet individual design point pH and conductivity conditions using either 6 M HCl or 2.4 M Tris buffers for pH adjustment and 1 M NaCl solution for conductivity adjustment. Twenty Centri-columns (one for each experimental condition) containing 200 uL each of mixed-mode AEX/HIC resin were obtained from Atoll GmbH (Weingarten, Germany). All 20 columns were run simultaneously in a 96-well plate format; columns were seated above 2 mL deep-well plates (Thermo Scientific, Waltham MA, USA) which were used for collection of volumes flowing through the column. Up to 1 mL of liquid was loaded into the top of each centri-column at a time. Flow of liquid through the column was induced by centrifugation of the column tray and deep-well plate for 1 minute at 600 rpm.

All centri-columns were equilibrated by flowing 5 CV's of EQ buffer (30 mM BisTris, pH and conductivity corresponding to individual experimental point conditions) through the 200 uL of resin. Samples were loaded onto their respective columns up to the limits specified by the experimental framework. Flow-through volumes during loading were collected and stored. The columns were washed with 5 CV's of EQ buffer, which was then pooled with the flow-through volume. Columns were stripped with 3 CV's of 75 mM acetate buffer, pH 3.00, 0.6 mS/cm, and then sanitized with 4 CV's of 1 M NaOH solution. Flow-through pools for all 20 run conditions were analyzed for mAb A titer using ProG-HPLC assays. Yield results based on titer values were input into the DesignExpert software in order to create prediction models and map parameter effects.

Mixed-mode lab-scale screening runs were performed on a 0.66 cm diameter column packed to a bed height of 10.7 cm. Samples of CEX eluate were adjusted to the desired pH and conductivity by the addition of either 25% acetic acid or 2.4 M Tris buffer, and 1 M NaCl. For all three runs conducted, the column was first equilibrated with EQ buffer (30 mM

BisTris, pH and salt concentration based on desired conditions). Sample was loaded onto the column to the desired mass loading level for each individual screening run. The column was then washed with 5 CV's of EQ buffer, stripped with 3 CV's of 75 mM acetate pH 3.00 buffer (acid regeneration buffer), and sanitized with 4 CV's of 1 M NaOH solution before being equilibrated for the next run. Load flow-through and wash pools for each run were collected. All three runs were conducted at a flow rate of 0.61 mL/min, corresponding to a residence time of 6 minutes.

The HIC run included in this experiment was performed on a 0.66 cm column packed to 11.9 cm with HIC resin. A sample of CEX eluate from the same pool used for mixed-mode runs was adjusted to pH 6.0, 20.5 mS/cm using 2.4 M Tris and 1 M NaCl solutions. The HIC column was first equilibrated with 5 CV's of running buffer (30 mM BisTris, pH 6.0, 20.5 mS/cm). The HIC column was loaded to 100 grams of mAb A per liter of resin. Five CV's of wash with EQ buffer were collected and pooled along with the sample load flow-through. The column was stripped using water, and then sanitized with 1 M NaOH. All phases of the run were conducted at a flow rate of 0.68 mL/min to achieve a residence time of 6 minutes. ProG-HPLC and SEC-HPLC assays were conducted on each mixed-mode flow-through pool and the HIC flow-through pool to determine yield and aggregate clearance of each screening run.

6.1.4 – Analytical Assays

Titer measurements for mAb A process samples were obtained with a Protein G – HPLC assay. A 30 mm x 2.1 mm POROS Protein G column (Applied Biosystems, Carlsbad CA, USA) was fitted to a Waters e2695 liquid chromatography system (Waters Corp., Milford MA, USA). Volume of each sample injection was set to correspond with a mass injection of

100 ug mAb A. A mobile phase consisting of 25 mM sodium phosphate, 200 mm sodium chloride, pH 6.5 was used during column equilibration and sample injection. Samples were eluted off the column using 200 mM NaCl, pH 3.0 buffer. Flow rate was set at 2.0 mL/min. Sample elution peaks were detected by absorbance readings at 280 nm. Peak areas were determined via integration and plugged into standard concentration calibration curves in order to calculate mAb A concentration present within the sample.

HMW values for mAb A samples were obtained using a Waters e2695 system fitted with a TSK Gel G3000 SW (300 mm x 8 mm) size exclusion column (Tosoh Bioscience, King of Prussia PA, USA). Volume of each sample injection was set to correspond with a mAb A mass injection of 100 ug. 100 mM sodium phosphate, 200 mM NaCl, pH 6.8 running buffer was used for each sample at a flow rate of 1.0 mL/min. Method duration for mAb A sample runs was set to 17 minutes. Elution peaks were detected using absorbance at 280 nm, and manually integrated to determine the proportion of total peak area attributed to high molecular weight aggregates.

HCP concentrations in mAb A process samples were determined using an in-house ELISA assay which utilizes electrochemiluminescence (ECL). Process samples were diluted appropriately in buffer (1.0 % bovine serum albumin (BSA), 1.5% Tween-20 in 1X Phosphate Buffered Saline (PBS)) such that each dilution would read within the assay range (8 – 425 ng/mL). Streptavidin-coated ECL plates (Meso Scale Discovery, Rockville MD, USA) were blocked with 25 uL of 3% BSA solution, incubated/shaken at room temperature for 30 to 60 minutes, then decanted to remove excess blocking solution. Plate wells were filled with 25 uL of sample. 50 uL of biotinylated and Sulfo-tag labelled anti-CHO HCP antibody solution were then added to each well. Following this, the plates were incubated at room temperature and agitated at medium speed for 4 to 5 hours. Plates were then washed three

times with 300 uL of 1X PBS, 0.05% BSA solution. 150 uL of 2X Read Buffer T (Meso Scale Discovery) were added to each well. Plates were read using a Sector Imager 6000 plate reader (Meso Scale Discovery). Emission of samples at 620 nm was measured and plugged into standard calibration curves to determine HCP concentration of unknown process samples.

DNA concentrations in process samples were determined using a repeat Q-PCR (quantitative polymerase chain reaction) assay. Samples were first diluted in 1X PBS, 0.5 M NaCl buffer if necessary. A MagMAX Express 96 (Applied Biosystems) instrument and associated equipment was used to extract and elute DNA from process samples. DNA extraction and elution from treated sample was performed using lysis buffer and elution buffer obtained from a “PrepSEQ Residual DNA Analysis” kit (Applied Bioscience). Following DNA extraction, samples were analyzed for DNA concentration using a Prism SDS 7300 workstation (Applied Biosystems). 25 uL of sample DNA extraction solution were transferred to wells on a 96-well Q-PCR plate. 25 uL of PCR reaction mix (Applied Biosystems) were added to these wells. The solution in each well of the 96-well plate was mixed thoroughly before the entire plate was centrifuged at 2000 rpm for 2 minutes. Plates were manipulated and analyzed on the SDS 7300 using standard, built-in Q-PCR procedure in order to determine DNA concentration present within each well.

6.2 – Results and Discussion

6.2.1– AEX Condition Screening

Anion exchange chromatography in flow-through mode is a logical choice for the first purification step following depth filtration, because the product stream is already in suitable pH and ionic strength conditions (pH 6.5, 2.0 mS/cm). Flowing depth filtrate

through at these conditions allows the majority of negatively charged impurities (e.g. DNA and acidic HCP's) to bind to the stationary resin/membrane while mAb A, which has a net neutral charge at a pH so close to its isoelectric point, flows unbound through the column [37]. Aggregated species and other product charge variants will also bind to the stationary phase at this pH, while salt concentration is low enough to prohibit competitive binding by free ions in solution [38].

Two different types of anion exchange purification schemes were evaluated to determine their yield and and impurity clearance capabilities. One is a traditional strong anion exchange resin used in Biogen Idec's purification platform for antibodies. The other is an AEX membrane that has been designed to have a high operating flow rate, and advertises impurity clearance comparable to AEX chromatography resins. Anion exchange membranes are attractive from an economic standpoint due to their high flow rates, decreased cycle times, and increased throughput. Membranes have high impurity binding capacities due to their convective pore structure, which can bind larger components (such as plasmids and virus particles) irrespective of high flow rates [39].

Re-solubilized mAb A material at pH 6.5, 2.0 mS/cm was low-pH adjusted in order to reduce turbidity and facilitate loading onto the AEX column/membrane. Low pH adjustment in lieu of depth filtration was conducted for ease of load sample preparation. Figures 6.1 and 6.2 below show the chromatographs for AEX in flow-through and AEX fast-flow membrane in flow-through.

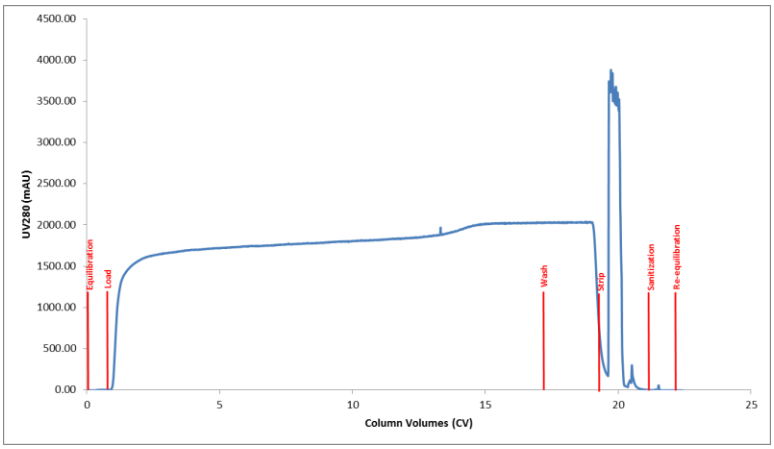

Figure 6.1: AEX in flow-through chromatograph. The blue trace depicts UV280 absorbance values (mAU) vs. volume flowed through the column in column volume (CV) multiples. Red vertical markers denote the beginning of phases (equilibration, load, wash, strip, sanitization, re-equilibration).

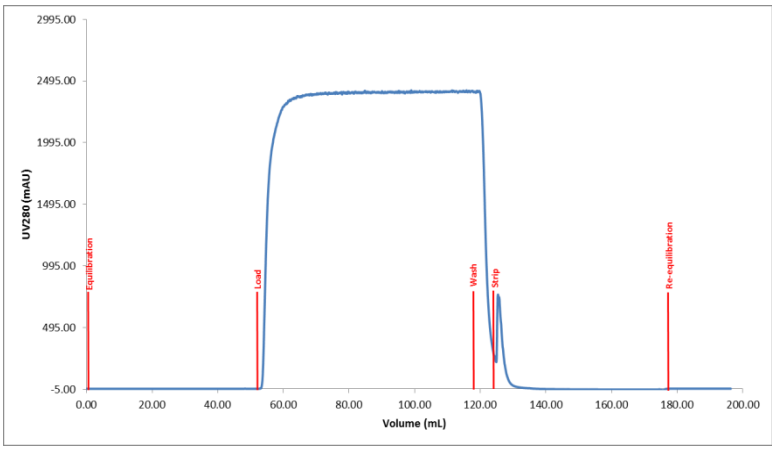

Figure 6.2: AEX fast-flow membrane in flow-through chromatograph. The blue trace depicts UV280 absorbance values (mAU) vs. volume flowed through the membrane (mL). Red vertical markers denote the beginning of phases (equilibration, load, wash, strip, re-equilibration).

Both chromatographs appear as expected – the UV280 trace shows mAb A flow-through during the sample loading stage in both figures. For each purification step, fractions were collected at various loading levels to determine impurity clearance performance as a function of product load. Table 6.1 shows the results of this purification study for the two steps described above. Yields for all fractions collected from both schemes were greater than 80%. Step yields increase as loading increases, which allows impurities to replace any weakly-bound product on the resin/membrane. From this data, it is apparent that both AEX flow-through and the AEX fast-flow membrane final flow-through pools have very little residual DNA. Although the low pH adjustment removed the bulk of the DNA before the sample was loaded onto either purification medium, both operations brought the DNA level to below the lower limit of quantification for the assay. It is thought that the optimized depth filtration sequence determined earlier will provide a similar level of DNA clearance.

The HCP levels across these two purification modes were quite different. The AEX resin provided an approximate 1.3 log reduction of HCP even at 400 g/L resin loading. Log reduction is calculated by taking the log of the ratio of HCP concentration in the load to HCP concentration in the flow-through pool. It appears the membrane barely provided any HCP clearance even at the lowest load density. AEX resin provides a ~50% reduction in high molecular weight content, whereas AEX membrane does not provide significant aggregate clearance.

Table 6.1: AEX condition screening experiment impurity profile.

Sample	HMW (%)	HCP (ppm)	DNA (ppb)	Cumul. Yield (%)
Re-solubilized Precipitate	---	209582	588381	---
AEX Resin Load	3.00	20360	10	---
AEX Resin 200 g/L Fraction	1.54	1211	< 1	84.6
AEX Resin 400 g/L Fraction	1.22	902	2	91.6
AEX Membrane Load	3.00	20360	10	---
AEX Membrane 2 g/mL Fraction	2.63	13155	2	79.6
AEX Membrane 4 g/mL Fraction	2.90	24995	< 1	88.7
AEX Membrane 5 g/mL Fraction	2.75	17287	< 1	90.9

Based on these results, it was decided that AEX resin in flow-through mode would be utilized as the first purification column operation, due to its high performance in impurity reduction. Although including the AEX fast-flow membrane step in the process would offer significant advantages, such as a reduction in processing time and the ability to load higher levels of impurities onto the membrane in flow-through mode [40], it did not perform as well as AEX resin in HCP clearance and thus was not a feasible option. Lesser HCP and HMW% clearance when using the AEX fast flow membrane may be due to low residence time of load material on the membrane. At a flow rate of 2.4 mL/min, the residence time across the membrane is approximately 0.03 minutes, which is much lower than the 6 minute residence time seen by the AEX resin column operation. The flow rate for the fast-flow membrane was set according to manufacturer recommendations. Increasing the residence time on the membrane would likely improve HCP reduction, but compromises the fast-flow aspects that make the membrane attractive as a purification step.

6.2.2 – CEX Condition Screening

The next objective in developing the purification process was to determine ideal conditions for the second column purification step, chosen to be cation exchange chromatography in bind/elute mode. Studies have shown that CEX is a powerful tool for HCP reduction, and that newer generation high-capacity CEX resins have broad applicability to a variety of antibody products. One such resin, proven to have a high dynamic binding capacity for mAb A, was used for this study [41]. CEX chromatography relies on positively-charged product binding to the negatively-charged resin while negative or neutral impurities flow-through. The operating conditions for a CEX run must be chosen carefully to achieve this effect. Ideally, pH of the column load must be below the product's isoelectric point in order to make the mAb molecules positively charged. Lower conductivity of the load for this type of bind/elute mechanism is desired, because there will be fewer ions to compete with mAb product for resin binding sites.

Screening for the CEX operation was performed at three pH conditions: pH 5.0, 5.5, and 6.0. All screening runs were performed at the same column loading: 70 g/L. This loading level was chosen based on previous optimization experiments for mAb A. The conductivity was kept at 5 mS/cm to preserve high product binding at these pH values. Although low salt conditions are ideal for CEX, this conductivity value was chosen for screening because studies have shown that some base level of salt is needed in the load to shield strong positive antibody charges that can repel other antibody molecules [3]. Antibody binding to CEX resin shows an initial increase in capacity with increasing salt strength as this repulsion mechanism is counteracted. This is followed by the eventual decrease in capacity due to charge competition for resin binding locations [3]. The load material was prepared by sending re-solubilized precipitate in low salt buffer though an X0HC depth filter, and then adjusting to appropriate load pH and conductivity conditions.

Although CEX is being considered for the second column purification step after AEX in FT, the decision was made to determine the optimal CEX conditions using just X0HC-depth filtered material as load, not material that has been sent through the full depth filtration process and the AEX step. The latter condition would be more indicative of the eventual proposed final process conditions, but the former condition presents a worst-case scenario (and thus a greater impurity challenge) for the CEX step.

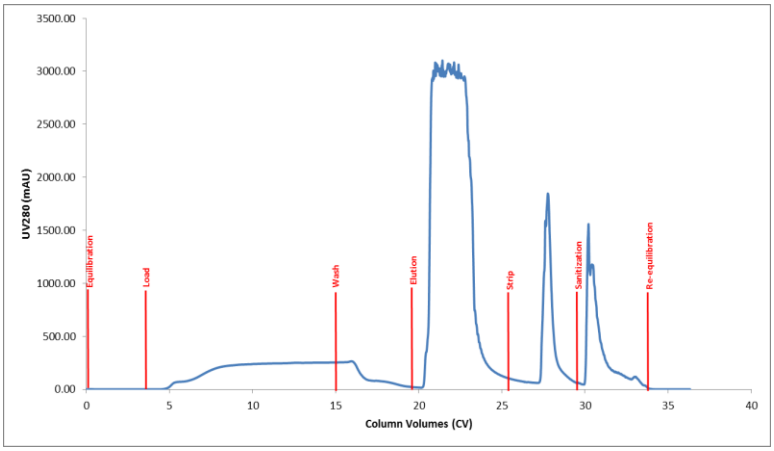

Figure 6.3: Representative chromatograph for CEX in bind/elute mode. pH 5.0, 5.0 mS/cm run shown. The blue trace depicts UV280 absorbance values (mAU) vs. volume flowed through the column in CV multiples. Red vertical markers denote the beginning of phases (equilibration, load, wash, elution, strip, sanitization, re-equilibration).

Figure 6.3 shows a representative chromatograph for the CEX runs. Table 6.2 gives analytical data (HCP, HMW%, and yield) for each of the three CEX runs. A DNA analysis was not conducted for these samples, as it is understood that the AEX step which will precede the CEX step in the final process essentially eliminates any residual DNA (see Table 5.6). Step yields for the pH 5.0 and pH 5.5 runs are as expected, both greater than 90%. The pH 6.0 run had poor yield due to product loss during the sample load stage, as binding capacity is reduced with increasing pH.

Table 6.2: CEX condition screening analytical data.

Sample	mAb A Titer (g/L)	HMW (%)	HCP (ppm)	Yield (%)
CEX pH 5.0 Run Load	6.17	2.40	40991	---
CEX pH 5.0 Run Elution	16.61	3.14	1331	92.9
CEX pH 5.5 Run Load	6.17	2.46	41524	---
CEX pH 5.5 Run Elution	16.51	3.59	618	92.3
CEX pH 6.0 Run Load	6.14	2.35	43832	---
CEX pH 6.0 Run Elution	10.56	5.00	657	59.6

The HCP removal of the CEX step for all three conditions was very good, bringing the HCP down from ~40k ppm to less than 1500 ppm. Including a bind/elute step in the final process gives the added advantage of concentrating the product stream. Elution titer is nearly triple the load titer for the pH 5.0 and 5.5 runs. Increasing concentration at this stage of the process will reduce processing times and volume requirements for future purification operations.

An interesting trend was noticed with the HMW% values for the three CEX runs. It appears that the aggregate level increased across the CEX step in all three cases, from the load, approximately 2.40%, to varying levels between 3.14% and 5.00%. It also appears that elution aggregate levels increase in direct correlation with the pH of the run, as the pH 6.0 run had the highest final aggregate level (5.00%), while the pH 5.0 run had the lowest aggregate level (3.14%). Increase in aggregation levels across a CEX bind and elute step is not an uncommon problem, and can be influence by strength of binding between mAb and resin, as well as elution salt type (among other factors) [42].

Further experiments were conducted to determine why CEX eluates from the condition screening experiment show large increases in aggregation levels. It is thought that recovered mAb A precipitate material will have a higher starting aggregate level than non-precipitated material (HCCF), due to some residual precipitates not being completely restored to monomer form during re-solubilization. It may be the case that the CEX step itself is causing aggregation of product. Studies evaluating high-capacity CEX chromatography as a direct antibody capture step have shown that strong binding conditions for antibody product on CEX resin can cause aggregation [41]. Also, the precipitation and re-solubilization process may render the antibody product more prone to aggregation, as product could have a tendency to revert back to its aggregated state even after re-solubilization.

Comparison of mAb A HCCF material over CEX versus precipitate material over CEX, both at strong and weak antibody binding conditions, will shed some light on the issues discussed above. An additional difficulty is encountered when attempting to assay highly impure material. Samples that have high turbidity or high HCP contents run the risk of fouling the SEC-HPLC column used to quantify aggregate levels. It is therefore unfeasible to accurately assay re-solubilized mAb A precipitate pre-depth filtration, and assaying of mAb A HCCF is avoided as well. For this reason, both mAb A HCCF and re-solubilized precipitate after depth filtration were sent through a Protein A column in order to reduce impurity content. The nature of Protein A causes impurity clearance without significant aggregate reduction, as aggregate compounds still have strong affinity for the resin. HCCF after Protein A had an aggregate level of 2.07%, while precipitate material had an aggregate level of 3.22%. This confirms the theory that re-solubilized precipitate material has higher initial aggregation content compared to harvest material.

To investigate the effect strength of mAb A binding to CEX resin has on aggregate formation, HCCF – ProA eluate was taken over CEX at strong binding conditions (pH 4.6, 5.0 mS/cm) and at relatively weaker binding conditions (pH 4.6, 12.5 mS/cm). Electrostatic interactions between antibody molecules increase in strength as pH is lowered and ionic strength of the solution is decreased. To build a comparison to mAb A precipitate, representative process material (re-solubilized precipitate following depth filtration and AEX in FT) was taken over CEX at the same two conditions, plus the optimized pH 5.5, 5.0 mS/cm condition determined earlier. Table 6.3 shows the aggregate values obtained at each stage along with HCP assay results for precipitate samples.

Table 6.3: HMW% values for aggregate investigation runs.

CEX Load Sample Type	CEX Run pH	CEX Run Conductivity (mS/cm)	Pre-CEX HMW %	Post-CEX HMW %
HCCF	4.6	5.0	2.27	3.13
	4.6	12.5	2.07	2.18
Precipitate	5.5	5.0	1.56	2.85
	4.6	5.0	1.56	5.08
	4.6	12.5	1.56	2.07

*Samples not submitted for HCP assay

The HCCF sample taken over a CEX column at strong binding condition (pH 4.6, 5.0 mS/cm) shows an increase in aggregate content. This is consistent with the theory that strong binding can induce aggregation across the CEX step. Precipitate samples at the same conditions also show an increase in aggregation levels, although this effect is more extreme as the HMW% post-CEX more than doubles. HCCF over CEX at relatively weaker binding conditions (pH 4.6, 12.5 mS/cm) does not cause any significant increase in aggregation. The precipitate analog for this condition does see a slight aggregate increase, but not as pronounced as for strong binding conditions. Comparison of aggregate increases between

HCCF and precipitate material indicates that precipitate material, under aggregate-inducing conditions, is more likely to see a greater increase in aggregation. As hypothesized earlier, this may be because product post-precipitation is prone to re-aggregation due to newly exposed hydrophobic groups or some similar structural change.

Yields for all 5 CEX runs shown in Table 6.3 are greater than 93%. HCP content of the load for all precipitate conditions screened was constant at approximately 2000 ppm. There was no significant difference in HCP clearance between the new best-case precipitate CEX condition (pH 4.6, 12.5 mS/cm) and the other two precipitate conditions screened. Since these new conditions prove effective for product retention and HCP clearance while keeping aggregate increase relatively low, pH 4.5 and 12.5 mS/cm were chosen as the operating conditions for the CEX purification step.

6.2.3 – Mixed-mode Condition Optimization

Up to this point, conditions for three out of the four unit operations that will comprise the purification process following PEG/$ZnCl_2$ precipitation have been defined. While the HCP and DNA concentrations of the product stream following the CEX step are relatively low, data has shown that CEX eluate contains unacceptable levels of high molecular weight aggregates. The fourth purification step, chosen to be mixed-mode anion exchange/hydrophobic interaction chromatography in flow-through mode, will ideally eliminate these aggregates while providing some additional impurity clearance.

In traditional mAb purification processes, hydrophobic interaction chromatography is often used for aggregate reduction [43]. As an alternative to these HIC resins, industry is recently turning to mixed-mode resins that combine hydrophobic, ionic, and hydrogen bonding components, as they provide greater purification efficiency due to their antagonistic ligand

properties. When working with resins that rely on multiple different interactions to purify product, dedicated optimization work is required to identify running conditions that will give the desired impurity clearance while avoiding large amounts of product loss. The parameters most often scrutinized when running mixed-mode chromatography resins in flow-through mode are pH, salt concentration, and loading of the column in flow-through. All three of these parameters will affect the physical-chemical interactions between the resin, mAb product, and any impurities that are present in the product stream. In order to fully understand the effects of these parameters on unit operation yield, a high throughput design of experiments (DOE) study was conducted using small-scale mixed-mode centri-columns. Based on this high throughput screening, potential high yielding run conditions were identified and further screened on lab-scale columns for aggregate reduction performance in order to identify conditions suitable for inclusion in the final process.

DOE for high throughput mixed-mode screening was conducted using DesignExpert software. A 2^3 factorial design with two replicates and 4 midpoints (20 points in total) was used as the framework for the study. Three parameters were incorporated, in a similar fashion to high throughput resin screening work conducted by Connell-Crowley et al [44]. Load salt concentrations were varied between 100 mM and 200 mM sodium chloride, load pH values were varied between 5.0 and 6.5, and resin loading was varied between 50 and 250 grams of mAb A per liter of resin. Atoll centri-columns pre-packed with 200uL of AEX/HIC resin were chosen as the high throughput platform on which the DOE runs were performed because of their ease of use and quick run times.

Centri-column flow-through pools were analyzed for mAb A titer, and step yield values were calculated for each combination of pH, conductivity, and resin loading screened. The low residence time offered by the Atoll centri-columns (~10 seconds) during the product loading

stage does not make them suitable for analyzing impurity clearance. Table 6.4 shows the various combinations of parameters that were screened on the centri-columns, and the yield values associated with them. Each parameter combination was run on one separate centri-column. Figures 6.4 and 6.5 show 2-D yield contour plots laid over pH and conductivity ranges at 50 grams per liter and 250 grams per liter loading, respectively. Figure 6.6 shows a yield contour plot laid over resin loading and pH variables, keeping the salt concentration constant at 200 mM sodium chloride.

Table 6.4: DOE framework for mixed-mode resin screening. List of individual pH, conductivity, and resin loading conditions tested. Each condition was run on one Atoll Centri-column.

Order #	Salt Conc. (mM NaCl)	pH	Resin Loading (g/L)	Yield (%)
1	100	5.00	50	72.7
2	100	5.00	50	73.3
3	200	5.00	50	65.2
4	200	5.00	50	66.1
5	100	6.50	50	17.1
6	100	6.50	50	15.4
7	200	6.50	50	26.4
8	200	6.50	50	22.4
9	100	5.00	250	89.0
10	100	5.00	250	91.2
11	200	5.00	250	89.3
12	200	5.00	250	88.8
13	100	6.50	250	58.9
14	100	6.50	250	60.7
15	200	6.50	250	71.6
16	200	6.50	250	72.8
17	150	5.75	150	72.7
18	150	5.75	150	66.2
19	150	5.75	150	72.8
20	150	5.75	150	72.4

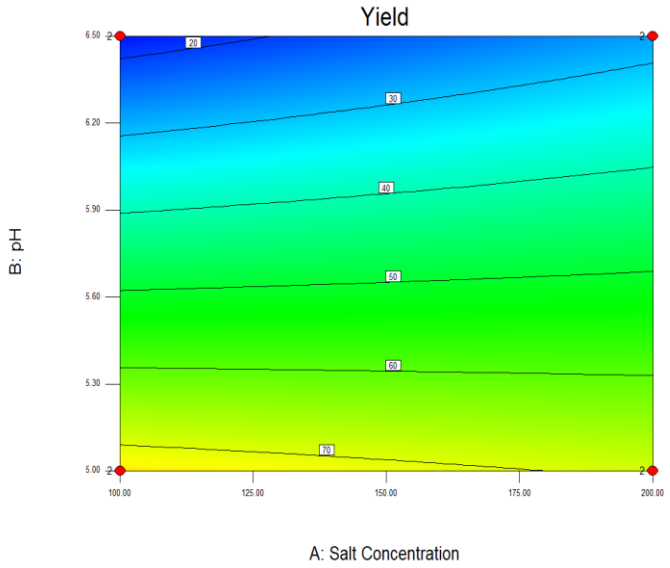

Figure 6.4: 2D yield contour plot at 50 g/L resin loading. Predicted yield values are plotted as a function of pH and salt concentration for resin loading at 50 g/L.

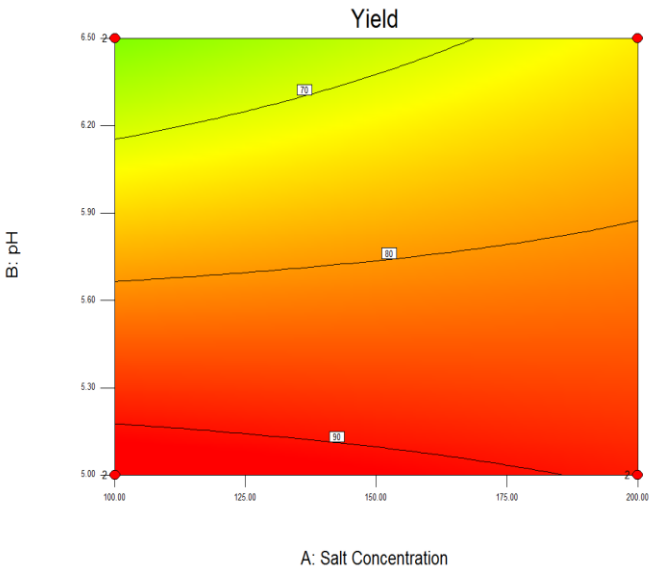

Figure 6.5: 2D yield contour plot at 250 g/L resin loading. Predicted yield values are plotted as a function of pH and salt concentration for resin loading at 250 g/L.

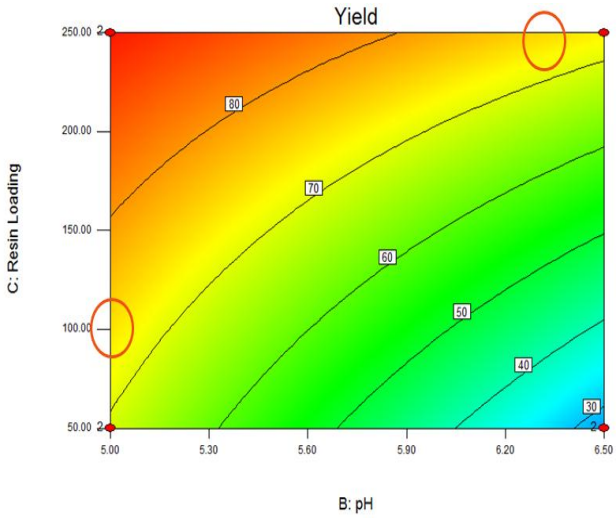

Figure 6.6: 2D Yield contour plot at 200 mM NaCl. Predicted yield values are plotted as a function of resin loading and pH for salt concentration held constant at 200 mM NaCl. Red circles denote the condition regions selected for lab-scale screening runs.

From Figures 6.4 and 6.5, it is evident that yield of the mixed-mode step is greatly influenced by pH of the load. Decreasing pH from 6.5 down to 5.0 results in approximately 50% more yield at 50 g/L loading, and closer to 20% more yield at 250 g/L loading. This is expected; mAb A has a stronger positive charge at lower pH's and thus is less likely to be retained by the anionic exchange properties of the resin. The two contour plots also show that salt concentration does not play a commanding role in determining yield. Figure 6.6 shows a contour plot of yield vs. resin loading and pH with the salt concentration kept constant at 200 mM sodium chloride (the salt concentration associated with the highest yields). This plot indicates that product recovery increases with increased loading onto the column across the entire pH range. Greater resin loadings in flow-through allow greater quantities of impurities to flow through the column alongside product. These impurities will compete with mAb A for binding sites on the resin, and any mAb A that is not bound or weakly bound to the resin will be bumped off and become retained in the flow-through

pool. The danger with high loading is that this effect may cause weakly-bound aggregates to come off the column as well, so loading limit must be decided carefully to achieve a balance between purification potential and step yield.

Taking these results into account, two potential run conditions were selected for evaluation of aggregate removal capability at lab-scale. Resin loading and pH values were selected such that both conditions would achieve approximately 75% yield. Salt concentration was held constant at 200 mM NaCl. It is recognized that yield results, when conditions are screened on a lab-scale column as opposed to high-throughput mode, will be greater by approximately 10% to 20% due to longer residence time and controlled flow through the column. The red circles on Figure 6.6 correspond to target areas for run condition selection. The first condition selected was pH 5.0, 200 mM NaCl, 110 g/L resin loading, and the second condition selected was pH 6.3, 200 mM NaCl, 250 g/L resin loading. CEX eluate generated from re-solubilized mAb precipitate that had been depth filtered was used as load material for both runs. Figures 6.7 and 6.8 display the chromatographs for both screening runs. Table 6.5 gives the associated yield and HMW% assay values.

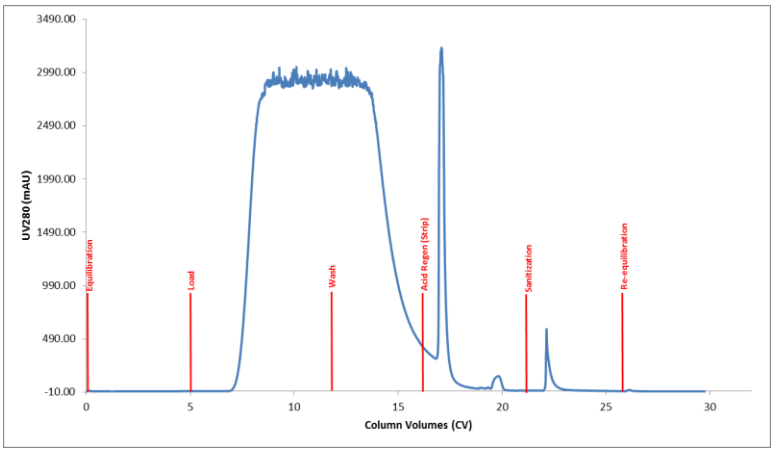

Figure 6.7: Mixed-mode column screening at pH 5.0, 200 mM NaCl, 110 g/L loading. The blue trace depicts UV280 absorbance values (mAU) vs. volume flowed through the column in CV multiples. Red vertical markers denote the beginning of phases (equilibration, load, wash, acid regen (strip), sanitization, re-equilibration).

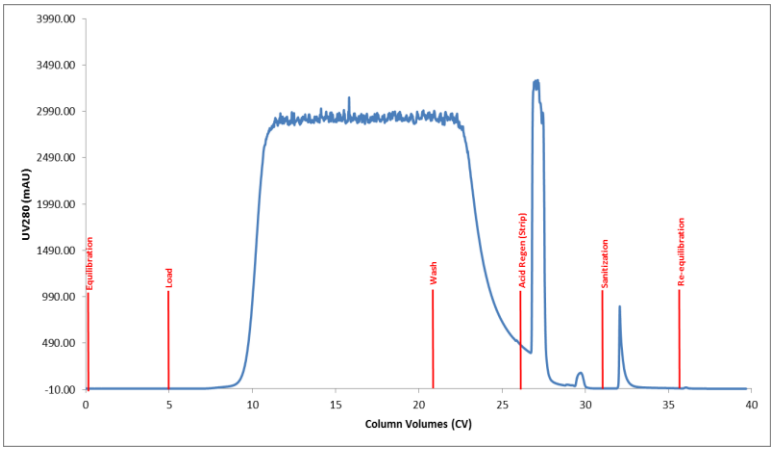

Figure 6.8: Mixed-mode column screening at pH 6.3, 200 mM NaCl, 250 g/L loading. The blue trace depicts UV280 absorbance values (mAU) vs. volume flowed through the column in CV multiples. Red vertical markers denote the beginning of phases (equilibration, load, wash, acid regen (strip), sanitization, re-equilibration).

Table 6.5: Yield and HMW% data for mixed-mode column screening runs. Salt concentration is 200 mM NaCl in both cases.

Sample	HMW %	Yield (%)
Mixed-mode Load	3.60	---
pH 5.0, 110 g/L Loading	2.71	89.9
pH 6.3, 250 g/L Loading	3.11	86.6

Both chromatographs show the ideal shape for a column operation in flow-through mode. Yield values for both screening runs were relatively high, and within the range predicted by the DOE results (~75% + 10% due to scale-up). However, neither running condition provided the desired level of aggregate reduction. Although the initial HMW% level present in the load for both runs was high (~3.60%), ideally the mixed-mode step should be able to reduce the HMW% down to below 1.0%. Further optimization of the run conditions for this mixed-mode step is needed.

Theoretically, lowering the loading limit of the mixed-mode column will result in better aggregate clearance. As discussed earlier, higher loading limits in flow-through essentially allow impurities such as remaining host cell proteins to flow through the column. These impurities can out-compete aggregates for binding spots on the resin, forcing weakly bound aggregates off the column and into the flow-through pool. Lowering the load limit on the column may help to counteract this and keep aggregates bound to the resin. A third screening run was conducted mimicking the conditions of the second pH 6.3, 200 mM NaCl run, but loading on the column was reduced to 100 g/L. This third mixed-mode run was conducted side-by-side with a traditional HIC in flow-through step at low salt conditions previously optimized for mAb A: pH 6.0, 200 mM NaCl, 100 g/L loading [45]. Figure 6.9 shows the chromatograph for the comparative HIC run, while Table 6.6 shows a side-by-side comparison with the mixed-mode run.

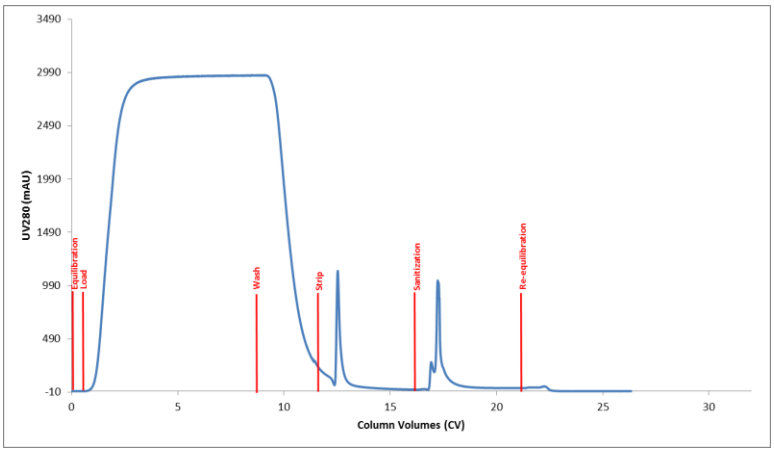

Figure 6.9: HIC in FT column screening at pH 6.0, 20.5 mS/cm, 100 g/L loading. The blue trace depicts UV280 absorbance values (mAU) vs. volume flowed through the column in CV multiples. Vertical markers denote the beginning of phases (equilibration, load, wash, strip, sanitization, re-equilibration).

Table 6.6: Final yield and HMW% data for mixed-mode and HIC column screening runs.

Sample	Load pH	Load Salt Conc. (mM NaCl)	Resin Loading (g/L)	HMW %	Yield (%)
Load Material	---	---	---	3.60	---
Mixed-mode FT	6.3	200	100	0.79	83.0
HIC FT	6.0	200	100	2.52	73.6

The results of this third mixed-mode screening run show that, as theorized, decreasing the amount loaded in flow-through results in better aggregate removal from the product stream. Aggregate now has been reduced by the optimized mixed-mode AEX/HIC step to 0.79%. Although the yield for this screening condition run was slightly lower than desired (82.97%), it was still higher than the DOE study predicted for this pH, salt and loading limit. HIC alone does not perform well in either yield or aggregate reduction, compared to the mixed-mode step. The combination of aggregate reduction and yield make mixed-mode

AEX/HIC chromatography at pH 6.3, 200 mM NaCl, and 100 g/L loading ideal for the final step in the PEG/$ZnCl_2$ purification process.

The work reviewed in Chapters 4, 5, and 6 mainly dealt with defining the unit operations and specific conditions incorporated within the proposed purification process for mAb A precipitate. Chapter 4 gave an explanation of how mAb A was precipitated using PEG and zinc chloride. Re-solubilization and subsequent dilution of this mAb precipitate yielded material which presented significant challenges for purification, namely high initial host cell protein content, unfilterable turbidity, and high aggregation levels. A depth filtration sequence, which combines C0HC and X0HC filtration in series, was inserted after re-solubilization to reduce the turbidity of the product stream while providing some initial HCP clearance. Screening studies were conducted to determine that anion exchange chromatography in flow-through mode was the ideal choice for the first column purification step. Results show that this chromatography step eliminates almost all residual DNA and provides a significant amount of HCP clearance as well. AEX in flow through was followed by cation exchange chromatography in bind/elute mode to further reduce host cell protein content while simultaneously concentrating the product stream. Finally, a DOE approach followed by lab-scale screening was utilized to determine prime running conditions for a mixed-mode AEX/HIC chromatography step, which takes care of the high aggregate levels remaining in the product. A summary of all operations in sequence and specific operating conditions can be found in the table below.

Table 6.7: Summary of process development work.

Operation	pH	Conductivity mS/cm	Loading
C0HC Filtration	6.5	2.0	1750 g/m^2
X0HC Filtration	6.5	2.0	530 g/m^2
AEX in FT	6.5	2.0	200 g/L
CEX in Bind/Elute	4.6	12.5	70 g/L
Mixed-mode in FT	6.3	20.5	100 g/L

What comes from these experiments is a series of steps that will, theoretically, come together to form a process capable of purifying mAb precipitate to acceptable standards. Although these unit operations provide the desired purification in isolation, it still remains to be seen whether they are able to function in combination and fully purify re-solubilized precipitate when put together. This work is the subject of Chapter 7, which deals with evaluating the proposed process as a whole.

CHAPTER 7 – FULL PROCESS RUN & PEG DETECTION ASSAY DEVELOPMENT

7.1 – Methods and Materials

7.1.1 – Full Process Run

Precipitate pellets containing mAb A product were re-solubilized in 100 mM Histidine buffer at a 1:1 pellet volume to buffer volume ratio. Pellets in buffer were mixed for ~24 hours until completely re-solubilized. The final mAb A re-solubilization pool was diluted in low salt buffer (30 mM BisTris, pH 6.5, 2.0 mS/cm) to an approximate concentration of 25 g/L. A 23 cm^2 C0HC depth filter was preconditioned by first flushing with water, then low salt buffer. The filter was loaded to ~1750 g/m^2 with re-solubilized mAb A product. Following this, the filter was flushed with 60mL of low salt buffer. Three 23 cm^2 X0HC filter were next preconditioned with water and low salt buffer. Each filter was loaded with C0HC filtrate to ~478 g/m^2 and flushed with 100mL of low salt buffer. All three X0HC filtrate pools were combined to form the final X0HC filtrate pool. This intermediate product was sent through a 0.22 micron filter (Thermo Scientific, Waltham MA, USA) before proceeding onto the rest of the process.

A 1.00 cm diameter chromatography column (Omnifit) was packed with anion exchange resin to a bed height of 12.9 cm in preparation for the AEX in FT step. The column was equilibrated with 5 CV's of low salt buffer, then loaded with depth filtrate corresponding to 200 grams of mAb A per liter of resin. Upon conclusion of the load phase, the column was washed with low salt buffer. The column was stripped with 1 M NaCl solution, then sanitized with 3 M NaCl, 0.5 M NaOH solution. All stages were run at a flow rate of 1.69 mL/minute, corresponding to a 6 minute residence time on the column. The product load

flow-through volume and wash volumes were pooled together to form the final AEX flow-through pool.

This AEX flow-through pool was adjusted to CEX load conditions, pH 4.6, 12.5 mS/cm, using 25% acetic acid and 1 M NaCl solution. CEX load material was 0.22 micron-filtered before proceeding. A 1.50 cm column (Omnifit) was packed to a bed height of 9.8 cm with CEX resin. The column was first equilibrated with 5 CV's of EQ buffer (50 mM sodium acetate, pH 4.6, 12.5 mS/cm). This was followed by column loading to 70 grams of mAb A per liter of resin. The column was then washed with EQ buffer before being eluted with 50 mM sodium acetate, 160 mM NaCl, pH 5.1, 18.77 mS/cm buffer. The column was then stripped with 1 M NaCl and sanitized with 0.5 M NaOH. Flow rate was held constant at 2.88 mL/min (6 minute residence time).

CEX eluate was adjusted using 0.9 M Tris, 0.24 M BisTris solution and 1M NaCl solution to match mixed-mode load conditions (pH 6.3, 21.5 mS/cm – corresponding to 200 mM NaCl) and then sent through a 0.22 micron filter. Mixed-mode AEX/HIC chromatography was performed on a 0.66 cm diameter column packed to a bed height of 10.7 cm. The column was first equilibrated with EQ buffer (30 mM BisTris, 200 mM NaCl, pH 6.3, 21.5 mS/cm). Product was loaded onto the column to approximately 100 grams of mAb A per liter of mixed-mode resin. The column was then washed with EQ buffer, stripped with 75 mM acetate, pH 3.00 buffer (acid regeneration buffer), and sanitized with 1 M NaOH solution. Flow rate was held constant at 0.61 mL/min (6 minute residence time). The flow-through volume during sample loading and the column wash volume were pooled together to form the final mixed-mode flow-through pool. All column bed heights were chosen such that column volumes were adequate for material processing purposes, while keeping a minimum bed height of 9 cm. Flow rates were varied such that a 6 minute residence time

was achieved on all columns. Final process samples as well as all process intermediates were assayed for titer to determine unit operation yield, using ProG-HPLC techniques. These samples were also assayed for HMW% by SEC-HPLC, and for HCP and DNA content by residual HCP ELISA assays and DNA assays.

7.1.2 – Free PEG Detection Assay

Detection of free residual PEG in final process material was carried out using a reversed-phase HPLC assay. Quantitative determination of free PEG in the presence of protein is challenging. Since PEG has very limited UV absorbance, traditional UV spectroscopy measurements are unable to produce a signal response when confronted with PEG. Instead, HPLC assay methods can be paired with more unconventional signal detectors. The assay discussed here utilized reversed-phase HPLC (RP-HPLC) with Corona charged aerosol detection (CAD) in order to measure residual PEG. Reversed-phase columns are packed with silica particles containing hydrophobic alkyl chains. Samples are passed through the column in a mobile phase that contains varying degrees of organic and aqueous solvents. Molecules and compounds present within the sample (such as mAb A and any residual PEG) will hydrophobically bind to the column in high aqueous mobile phases, and can be eluted from the column by switching to high organic mobile phases via a linear or stepwise gradient [46]. Compounds of greater hydrophobicity will elute later on in the gradient. Since mAb A and PEG have different degrees of hydrophobicity, it is possible to separate them in this manner.

When HPLC column effluent enters the CAD instrument, it is collected and immediately nebulized by a high-pressure stream of nitrogen gas. The eluent sample is then dried, and large droplets of solvent are sent to the drain while analyte particles present within the

sample are withheld. Nitrogen is passed by a corona wire, which imparts a strong positive charge onto the gas. From here, analyte particles are bombarded with this nitrogen flow. The positive charge is transferred to the particles, which then flow through an ion trap and into an ultra-sensitive electrometer. The charge on the analyte particles is measured and output as a voltage signal. Higher voltage signals correspond to higher charges, which typically indicate larger masses of analyte sample. By correlating mass (and therefore concentration) of analyte to voltage output, it becomes possible to determine unknown concentrations of analyte within samples by measuring voltage output.

An Agilent Series 1200 HPLC system (Agilent Technologies, Santa Clara CA, USA) was fitted with a 2.1 mm x 7.5 mm Zorbax Poroshell 300SB-C3 column (Agilent Technologies). Effluent from the column was passed through the HPLC UV detector before being sent through a Corona Charged Aerosol Detector (CAD) instrument (ESA, Chelmsford MA, USA). 0.1% triflouroacetic acid (TFA, Thermo Fisher, Waltham MA, USA) in HPLC-grade water (Thermo Fisher) was used as aqueous running buffer, and 0.1% TFA in acetonitrile (Thermo Fisher) was used as organic running buffer.

Nitrogen gas pressure to the CAD instrument was supplied via an in-house utility line. Range for CAD output was set at 500pA. The Poroshell C3 column and CAD system were first equilibrated by flowing 100% aqueous buffer for approximately 30 minutes through the entire system. The HPLC method for running a sample is as follows: column was equilibrated pre-sample injection for 5 minutes at 99% aqueous, 1% organic buffer. Injection volume of all samples was kept constant at 100 uL. Samples containing mAb A were diluted to a concentration of ~1 mg/mL before being injected. A linear gradient was run for the next 25 minutes, ramping aqueous buffer down from 99% to 15%. 100% organic

buffer, 0% aqueous buffer was run through the system for the next five minutes, followed by re-equilibration with 99% aqueous, 1% organic buffer.

PEG concentration standards for development of a calibration curve were made from dilutions of a stock 0.5 mg/L PEG in HPLC grade water solution, and run using the standard method described above. PEG peak area response by the CAD instrument was calculated by integrating the spike in output that occurs at approximately 16.15 minutes. A linear regression was calculated by plotting peak area response vs. PEG concentration, and the resulting regression equation was used to back-calculate residual PEG concentrations in unknown samples. End-of-process samples taken from the mixed-mode flow-through pool were sent through the assay for quantification. Antibody A material that was purified in a process involving no PEG was run as a control.

7.2 – Results and Discussion

7.2.1 – Full Process Run

Following the conclusion of all development work, a process consisting of four unit operations (depth filtration, AEX in FT, CEX in B/E, and mixed-mode AEX/HIC in FT) was designed. The overall objective of this process is to purify mAb A precipitate to the point where impurity levels are within acceptable standards, all while losing as little of the product as possible. While each individual unit operation had been tested for purification performance, the process as a whole has still yet to be tested. This section describes the results of such a “full process run”. Starting with solid mAb A precipitate material, the entire sequence of unit operations was performed in series to purify the product from this precipitated state into final process intermediate. Analytical data (HCP, DNA, HMW%, and yield assays) was taken at the conclusion of each individual step as well as at the final

process endpoint to monitor unit operation performance and to determine whether the final process material was sufficiently pure. Figures 7.1, 7.2, and 7.3 show chromatographs of the AEX in FT step, CEX bind/elute step, and mixed-mode AEX/HIC in FT step, respectively.

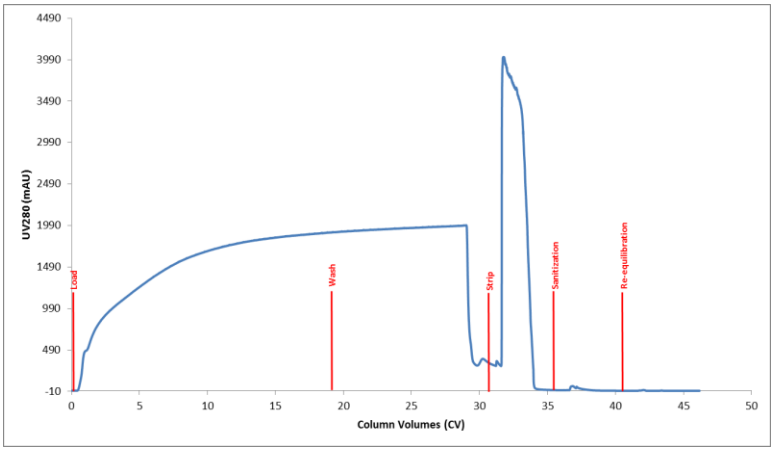

Figure 7.1: Full process run AEX in FT chromatograph. The blue trace depicts UV280 absorbance values (mAU) vs. volume flowed through the column in CV multiples. Vertical markers denote the beginning of phases (load, wash, strip, sanitization, re-equilibration).

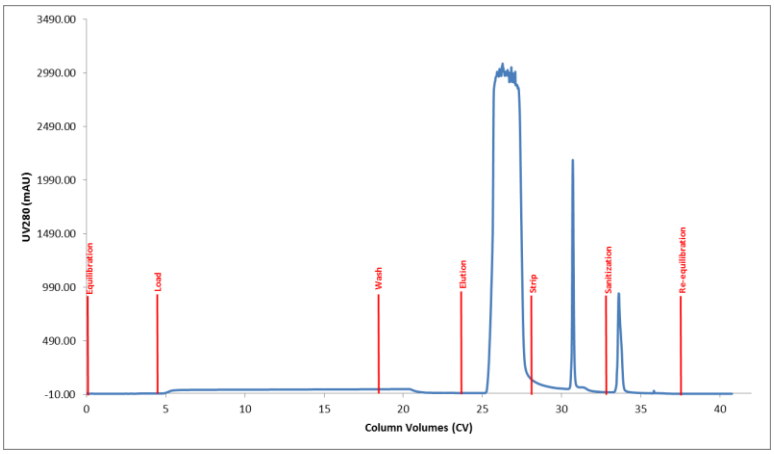

Figure 7.2: Full process run CEX in Bind/Elute chromatograph. The blue trace depicts UV280 absorbance values (mAU) vs. volume flowed through the column in CV multiples. Vertical markers denote the beginning of phases (equilibration, load, wash, elution, strip, sanitization, re-equilibration).

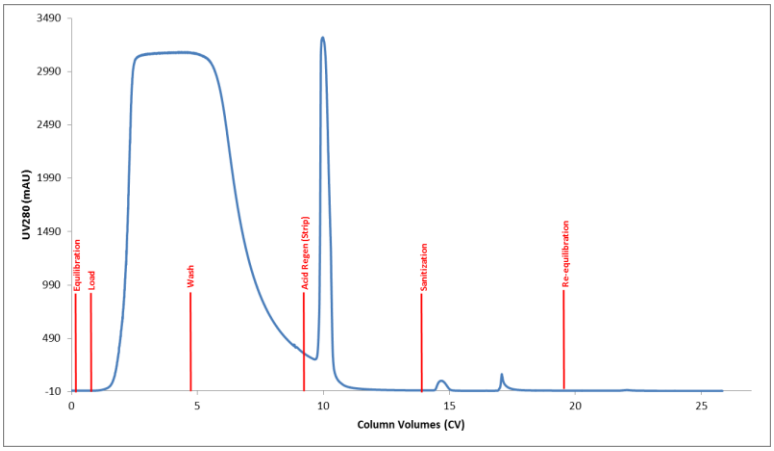

Figure 7.3: Full process run mixed-mode in FT chromatograph. The blue trace depicts UV280 absorbance values (mAU) vs. volume flowed through the column (mL). Vertical markers denote the beginning of phases (equilibration, load, wash, acid regen (strip), sanitization, re-equilibration).

Table 7.1: Full process run yield and analytical data. Residual HCP and DNA values for re-solubilized precipitate and C0HC filtrate are estimated from data gathered during previous development experiments.

Sample	mAb A Titer (g/L)	HMW %	HCP (ppm)	DNA (ppb)	Step Yield (%)
Re-solubilized Precipitate	23.11	N/A *	~100000	~590000	~100.0
C0HC Filtrate	18.93	N/A *	~100000	N/A **	98.9
X0HC Filtrate	7.00	N/A *	52541	631	87.1
AEX FT	5.12	1.57	1803	< 1	79.8
CEX Elution	27.99	2.03	85	< 1	96.4
Mixed-mode FT	10.11	0.67	56	< 1	89.6
Combined Yield	N/A	N/A	N/A	N/A	59.4

* HMW values not taken because sample was too turbid/impure to load onto SEC-HPLC system

** Sample not submitted for DNA assay

Table 7.1 summarizes the yield and impurity clearance performance of the process as a whole. Individual unit operation yields were approximately equal to what was predicted during developmental work, and the combination of all unit operations together resulted in an overall yield of approximately 60%. Three unit operations had yields below 90%: the X0HC depth filtration, AEX in FT chromatography, and mixed-mode AEX/HIC step. AEX in FT yield could possibly be improved if loading onto the column was increased. There is a danger of over-loading the column with impurities, which could result in breakthrough of HCP or DNA, so loading optimization studies are required to pinpoint the best target loading value. Studies have shown that mixed-mode chromatography, when run in flow-through mode, is greatly influenced by specific physical-chemical properties of individual mAb products [47]. Because of this, it is difficult to determine where the optimal loading capacity for mAb A lies. Although two screening runs were done at the same pH and conductivity conditions, one at 250 g/L loading and one at 100 g/L loading, additional runs could be performed to determine whether the optimal loading level lies somewhere between those

two endpoints. However, conditions must be carefully evaluated in order to ensure that increased step yield is not gained in sacrifice of essential aggregate removal capabilities.

Aggregate values for both the re-solubilized mAb A precipitate pool and either depth filtration pool were not taken for fear of fouling the SEC column used to conduct the assay. Previous experiments have shown that the initial aggregate level of re-solubilized material is somewhere between 3.00% and 3.50% (see Section 6.2.2), and that depth filtration does not provide any significant aggregate clearance. AEX in FT effectively halved HMW % following depth filtration. CEX eluate contained material that was slightly higher in aggregate level, as previously seen for pH 4.6, 12.5 mS/cm conditions. Mixed-mode AEX/HIC in flow-through reduced aggregate levels by approximately 67% to under the 1.00% threshold.

C0HC and X0HC filtrations in series provided an approximate 0.3 log clearance of HCP. The AEX step provided a significant amount of HCP clearance, bringing the value down to less than 2000 ppm. CEX in bind/elute further reduced the HCP content by 1.32 logs, which is similar to the performance capabilities reported elsewhere. Mixed-mode chromatography did not do much in the way of HCP clearance. As the product stream has already been through an anion exchange step, this half of the mixed-mode mechanism is not very effective at providing additional HCP reduction. Taking into consideration the fact that whatever impurities survived the AEX in FT step are unlikely to be eliminated by the mixed-mode resin, the 0.18 log reduction of HCP provided by this unit operation seems more reasonable. Finally, it appears as though the bulk of residual DNA is cleared by the depth filtration sequence and the AEX in flow-through step in tandem. These two operations bring the DNA down from the initial value of ~590k ppb in the load to less than 1 ppb, representing an approximate 5.77 log reduction factor.

Final process material will go through two additional steps that are standard for antibody platforms.. Following the mixed-mode FT step, the product stream will travel through a viral filtration step to remove any residual viral particles that remain in the process stream. Pore size of this filtration step is selected carefully so that virus particles (typically 18 – 26 nm in diameter) are excluded while product flows through the filter membrane. Due to the narrow pore size distribution characteristic of these filters, greater than 4 logs of viral clearance can be achieved while keeping yields greater than 99% [48]. Viral filtrate material is then sent through a UF/DF operation in order to concentrate product and buffer-exchange it into final formulation buffer. A 30 kilodalton cassette is utilized for this step. Product goes through 10 diafiltration volumes in order to ensure complete buffer exchange. At this point, the final product is ready to be filled into vials for distribution. Yield for ultrafiltration and diafiltration together is typically greater than 98%, while bulk filling operations have yields of approximately 99%. Including viral filtration, UF/DF, and bulk filling, the overall process yield is estimated to be 57.6% to 59.4%

7.2.2 – Free PEG Detection Assay

Although the PEG/ZnCl2 precipitation technology utilized here is a useful tool for decoupling upstream and downstream processing, the use of precipitation reagents to the product stream places an extra burden on the subsequent downstream process. In addition to clearing the traditional impurities associated with mammalian cell culture-based products, the four purification operations that have been discussed must also be capable of removing any precipitation reagents that remain in the product stream following precipitation. This focuses specifically on verifying the clearance of free, residual PEG.

After precipitation of the mAb product in the presence of free PEG occurs, the semi-solid antibody paste is sent through a centrifugation step. Here, PEG is excluded from the precipitated antibody product. This results in the formation of one phase that is rich in PEG (the centrifugation supernatant) and one phase without PEG (the harvested antibody precipitation pellet). Although there is a distinct phase separation that results in the clearance of the majority of PEG from the product stream, some residual PEG may still be harvested along with the mAb pellet.

The focus then shifts to how this residual PEG is removed from the product stream. There are multiple ways that PEG can be cleared, and some of these have already been incorporated into the process. The first method to remove residual PEG involves washing the pellet before re-solubilization. Essentially rinsing the pellet with a wash solution (either specific buffer or water) can clear residual PEG on the surface of the pellet. This has the added benefit of removing certain low molecular weight species as well, such as product fragments and host cell proteins. PEG can also be cleared via the incorporation of a CEX step in bind/elute mode. Product will bind to the resin, while uncharged residual PEG will flow directly through the column to waste. Multiple purification processes that aim to eliminate free PEG from pegylated protein products incorporate a CEX step for this very reason [49-51]. The inclusion of a final UF/DF step after mixed-mode AEX/HIC for buffer exchange purposes, as mentioned above, will help to eliminate any residual PEG that makes it past the CEX step. Pegylated protein products typically cite this final UF/DF operation as a mechanism for removing free PEG [52], [53]. Selection of an appropriate molecular weight cutoff for this UF/DF step is critical, as it is imperative that product be retained while low molecular weight species such as salts and PEG flow through the membrane. A MWCO of 30kDa is appropriate to remove PEG of the size used in this process.

A RP-HPLC assay with Corona CAD detection was developed to verify that final process samples do not have significant amounts of residual PEG. To determine whether a linear relationship between PEG concentration and Corona CAD output can be established, multiple standard concentration samples of PEG were run. Samples containing 0.5, 1, 2.5, 5, 10, 25, and 50 ug/mL of PEG were analyzed. Of these samples, no detectable voltage output could be obtained for the 0.5 and 1.0 ug/mL samples. Table 7.2 shows relevant data gathered from RP-HPLC analysis of these PEG standards. Figure 7.4, below, shows a plot of mass of PEG injected vs. Corona CAD peak response.

Table 7.2: RP-HPLC data for PEG concentration standards. Corona CAD response peaks were not detected for 0.5 and 1.0 ug/mL PEG samples.

PEG Concentration (ug/mL)	Injection Volume (uL)	Residence Time (min)	Response Peak Area (mV*sec)
0.5	100	peak not detected	peak not detected
1	100	peak not detected	peak not detected
2.5	100	16.17	57
5	100	16.16	132
10	100	16.16	337
25	100	16.17	988
50	100	16.18	1772

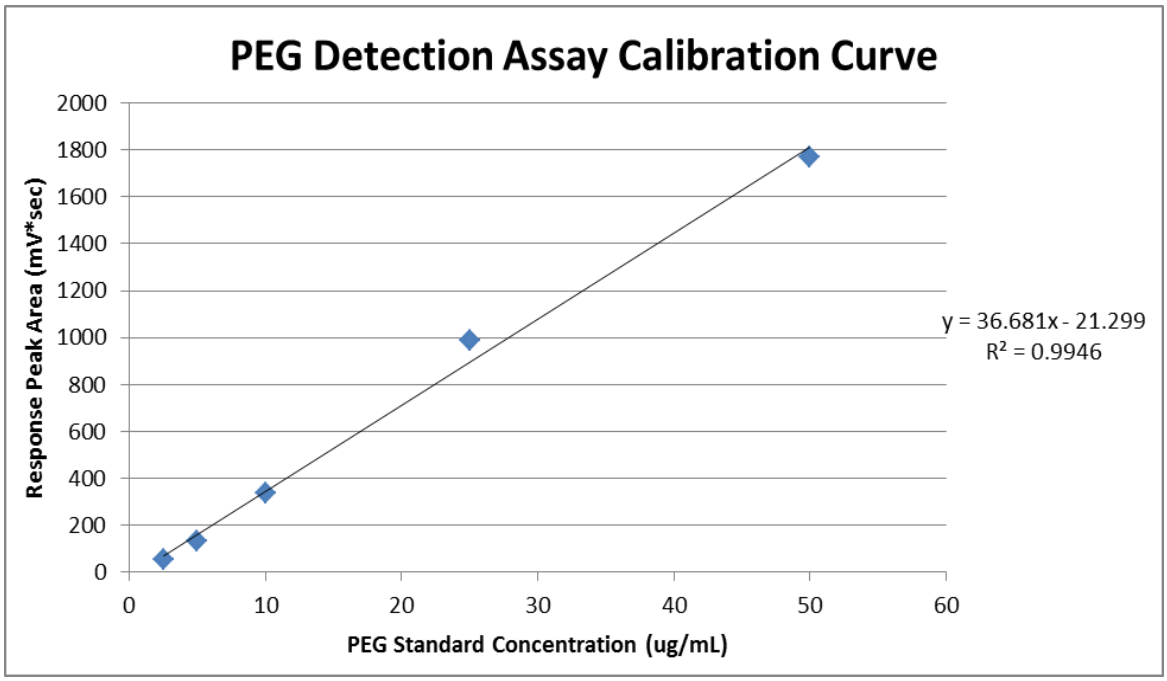

Figure 7.4: PEG concentration curve. Graph plots peak response vs. concentration of PEG standard injected. Range of the concentration curve extends from 2.5 ug/mL, the lowest concentration detected, to 50 ug/mL, the highest concentration tested.

Average retention time for PEG on the RP-HPLC column was approximately 16.15 minutes. Peak responses for PEG masses below 2.5 ug/mL were not produced by the Corona CAD instrument. Essentially, the lower limit for the assay is set at 2.5 micrograms per mL for this reason. The upper limit of the assay was kept at 50 ug/mL of PEG. Figure 7.4 illustrates that the relationship between peak response area and mass of PEG injected onto the column is highly linear. A regression fit to the data yielded the following equation:

$$[Peak\ Area] = 36.681 * [PEG\ Concentration] - 21.299$$

The R-squared value for this correlation is 0.9946, proving that the data has a high degree of linearity and that the assay is suitable for accurate detection of PEG within the 2.5 to 50 ug/mL range.

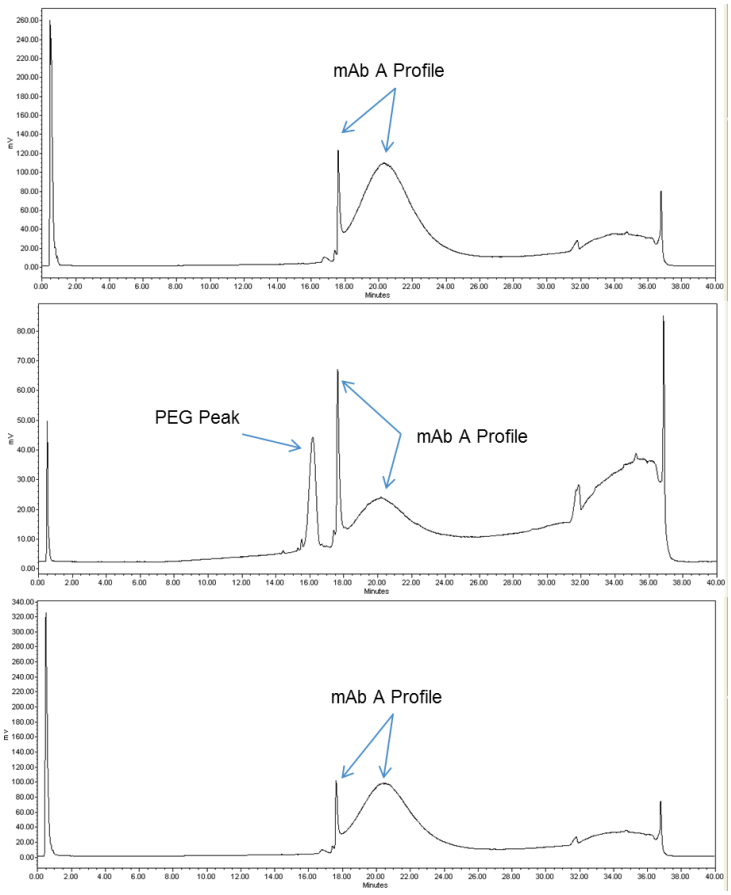

Figure 7.5: RP-HPLC chromatographs for PEG detection assay samples. All graphs show Corona CAD response (mV) vs. time (min). Top: Chromatograph for purified mAb A sample, sent through a non-PEG purification process. Middle: Purified mAb A sample spiked with 25 ug/mL of PEG. Bottom: Full Process Run final sample (mixed-mode flow-through).

Following assay calibration, various samples were analyzed. The top graph in Figure 7.5 shows the Corona CAD response of a sample of purified mAb A product, created using a non-PEG-based downstream process. There is a strong product signal associated with the mAb A product. This is characterized by a sharp peak eluting off the RP-HPLC column at approximately 18.00 minutes, that is then followed by a response envelope that spans the 18.25 to 24.00 minute marks. The tail end of this specific chromatograph shows additional peaks across the 31.00 to 37.00 minute marks, though to be due to pressure issues that occur when switching from 15% aqueous, 85% organic buffer directly to 0% aqueous, 100% organic buffer. These peaks also exist when evaluating HPLC-grade water "blank" sample response (not shown).

The middle chromatograph shows the CAD response for the same pure mAb A sample with PEG added to a concentration of 25 ug/mL. This illustrates the distinct separation between the PEG peak, which elutes at approximately 16.15 minutes, and the mAb A response profile which starts at 18.00 minutes. Pure mAb A spiked with a known sample of PEG proves that the assay is capable of distinguishing PEG from antibody product with sufficient resolution, and also provides a way to gauge the accuracy of the PEG calibration curve. Plugging the peak response area of the PEG signal into the calibration equation determined earlier gives an estimated PEG concentration of 27.77 ug/mL. Comparing this to the "true" value of 25 ug/mL yields an 11% error, which is within the recommended tolerance range of 20% for CAD instruments.

The bottom chromatograph of Figure7.5 displays the Corona CAD response for final process sample from the full process run. The mAb A response profile for this sample matches the pure product profile seen in the top chromatograph. No peak can be seen upon inspection of the typical PEG elution region (16.10 minutes). This leads to the conclusion that the final

process contains less-than-detectable quantities of PEG, corresponding to values of PEG less than 2.5 ug/mL. Dividing this limit by the concentration of the mAb sample (10.11 mg/mL), it is determined that the final process sample contains PEG quantities less than 250 parts per million.

CHAPTER 8 - CONCLUSION

8.1 – Final Evaluation of Process

Development of a downstream process designed to purify PEG/$ZnCl_2$ precipitated material has been discussed in the previous chapters. The end result is a process consisting of four unit operations in sequence: depth filtration, anion exchange chromatography, cation exchange chromatography, and mixed-mode AEX/HIC chromatography. These steps are followed by viral filtration and UF/DF steps included in the standard antibody purification platform. A downstream process is measured by its ability to isolate the target product while simultaneously eliminating potentially harmful impurities. To this end, four main parameters were monitored throughout process development: yield, residual HCP content, residual DNA content, and high molecular weight aggregate levels. Residual PEG concentration in final process samples was also determined in an effort to prove that the process is capable of clearing reagents added during the precipitation step.

Overall yield of the process was suitable, approximately 60%. While this statistic is in the lower end of the typical 60% to 80% yield range seen by mAb downstream processes [54], this is due to a combination of having to clear a concentrated impurity burden from precipitated material and not utilizing a traditional Protein A capture step. The overall lower cost of this non-Protein A process, combined with the high-throughput decoupling advantage that precipitation provides, helps to offset this difference in yield. The FDA recommends that final product HCP levels should be as low as possible, and that acceptance criteria should be set based on data from process development, preclinical and clinical trial material generation, and manufacturing consistency lots [24]. Most recombinant biopharmaceutical products have final HCP levels between 1 and 100 parts per million [25].

The FDA has suggested that final product contain no more than 100 picograms of cellular DNA per dose [26]. Typically, residual DNA assays have limits of quantitation between 1 to 10 pg/mL. Conversely, there is no overarching specification on the maximum allowable level for product aggregates. Some products may be stable at certain aggregate levels while other products may be adversely affected in terms of stability and safety. To account for this, manufacturers set control specifications on a product-to-product basis based on clinical lots, *in vitro* and *in vivo* studies, and individual product stability profiles [27]. Relevant data for mAb A suggests that a limit of 1.00% is suitable for HMW aggregates.

According to ICH guidelines, PEG is considered a process-related impurity and must be controlled as such. This involves either testing the final drug substance, or demonstration through suitable studies that the manufacturing process is able to control or reduce the process impurity to within acceptable levels [28]. Literature has examples of PEG detection assays that are used to quantify amounts of PEG in final product samples. These include similar RP-HPLC assays paired with Corona CAD instruments, and also SEC-HPLC assays paired with both Corona CAD and refractive index instruments. As previously mentioned, lower limits of quantitation for these assays are between 1.6 and 10 ug/mL. A typical control strategy for free PEG involves verifying that final drug product samples are below the lower limit of quantification for whichever assay is used.

Table 8.1: Comparison between final product impurity profile and final impurity industry specifications.

Impurity	Final Process Level	Industry Specification	Source for Specification
Host Cell Protein	56 ppm	< 100 ppm	FDA recommendation
DNA	< 5 pg/mL	< 100 pg/dose	FDA recommendation
HMW %	0.67%	< 1.00%	Internal Specification
Free PEG	< 2.5 ug/mL	< 2.5 ug/mL	Internal Specification

Table 8.1 shows that final impurity levels for the PEG/$ZnCl_2$ precipitation purification process meet general industry specifications for final HCP concentration. Final DNA concentration of the product is below 5 pg/mL. Dosage of mAb A is below 1 mL, meaning that final product meets DNA specifications of less than 100 pg/dose. Studies suggest that aggregate levels below 1.00% are considered safe and acceptable for mAb A. The process reduces aggregate to 0.67%, well below this limit. Final impurity values for this process are similar to those obtained by the traditional Protein A purification process for mAb A. Free PEG present in the final process sample is below the lower limit of quantitation for the detection assay, and below typical free PEG specifications for other drug products.

8.2 – Future Work and Potential Improvements

Multiple avenues for improvement were discovered during the course of process development. Further experimentation can be performed in order to increase overall yield of the process and also to increase impurity clearance of individual purification steps. A low pH adjustment of harvest material prior to concentration for PEG/$ZnCl_2$ precipitation can be conducted in order to reduce the turbidity and HCP load onto the eventual process. Adjusting the pH of the HCCF material to 5.5 will cause soluble impurities to undergo

isoelectric precipitation and flocculate out of solution, as was proven during process development work. Low pH adjustment of harvest material is not associated with large amounts of product loss (~ 5%). This adjusted material can then go through centrifugation in order to clear precipitated species. Depth filtration is another potential application for clarification of the adjusted harvest, if centrifugation is not an option for the manufacturing facility. Adjusting the harvest material before UF/DF and PEG/$ZnCl_2$ precipitation will reduce the amount of soluble impurities that are PEG-precipitated and subsequently re-solubilized. As such, this step will also reduce the impurity load on the C0HC-X0HC depth filtration sequence. This could potentially translate to increased loading onto both depth filters, which will improve yield and cost-effectiveness of the process.

Additional studies need to be performed to verify that the process developed here adequately clears virus particles from the product stream. The AEX in FT and CEX in bind/elute steps are expected to provide at least 5 and 3 logs of virus clearance, respectively [55], [56]. As mentioned before, greater than 4 logs of virus clearance can be expected from the viral filtration step. Based on these assumptions, the complete purification process will be able to provide adequate levels of viral clearance. However, if this is not the case, a low pH viral inactivation step can be introduced into the process. Dropping the pH of the product stream to within the 3 to 4 range and holding for 1 to 6 hours destroys virus particles by irreparably damaging their lipid layers and protein coats. Hold time for inactivation depends on the product and temperature conditions [18]. Low pH viral hold steps have been shown to provide greater than 4 logs of large-envelope viral inactivation [57]. Viral inactivation is typically included in mAb purification processes after Protein A chromatography, as the product stream is already at low-pH elution conditions. For the PEG/ZnCl2 precipitation process developed here, a low pH hold could be incorporated between the AEX in FT and CEX in bind/elute steps. Sufficient data would have

to be gathered to ensure that the product remains stable at low pH values for the duration of the hold step. Including another depth filtration after this proposed viral inactivation may reduce HCP content of the product stream further, while providing the added benefit of clearing any precipitates that form as a result of the low-pH hold.

Further work can be done to fully characterize the aggregate increase across the CEX bind/elute step. During initial screening it was observed that running the CEX step at increasing pH values (5.0, 5.5, 6.0) while keeping ionic strength constant at 5.0 mS/cm caused higher elution aggregate levels. Increased binding strength (which occurs at lower pH values) theoretically will result in higher aggregate levels; however results show that the opposite effect occurred. Attempting the CEX step at alternative conditions (pH 4.6, 12.5 mS/cm) defined previously for direct capture of mAb A from HCCF material determined that no aggregate increase occurred. A more thorough experiment can be performed where multiple pH and ionic strengths are screened to determine the underlying factor for aggregate generation across the CEX step.

Full process run results have indicated that the mixed-mode AEX/HIC purification step does not provide a significant amount of host cell protein clearance. Optimization of the mixed-mode step conducted during process development resulted in conditions which were successfully able to reduce aggregate content of the product below 1.00% while still maintaining high unit operation yield. However, this third purification step could be further improved to provide HCP clearance in addition to aggregate clearance. This will maximize the utility of this unit operation while ensuring that the final HCP concentration is well below the 100 ppm limit. Further screening of mixed-mode conditions can be conducted to gain HCP clearance – keeping pH and salt concentration constant at 6.3 and 200 mM NaCl (known to provide sufficient aggregate reduction) while reducing the column load in flow-

through may provide additional purification performance. HIC purification can also be optimized to see if it provides a more attractive alternative. The traditional HIC condition for mAb A (pH 6.0, 20.5 mS/cm, 100 g/L loading) was screened during process development; however this did not provide either as much aggregate clearance or yield as mixed-mode AEX/HIC. Varying pH, conductivity, and loading conditions for HIC in FT may provide both sufficient aggregate reduction and HCP reduction as well.

8.3 – Concluding Remarks

This thesis describes the design of a next-generation antibody purification process that integrates a protein precipitation technique as a decoupling step between upstream and downstream processing. The decoupling aspect of the PEG/ZnCl2 precipitation technology makes it possible to capture, freeze, and store an entire large-scale high-titer upstream harvest, eliminating the need for immediate downstream processing. The subsequent purification process confers several advantages over the traditional Protein A process used to purify antibody products. All three resins used in the next-generation process are lower in cost than Protein A resin, and are more chemically stable and easier to clean and regenerate/sanitize between batches. Elimination of the Protein A capture step, along with implementation of PEG/$ZnCl_2$ precipitation, essentially removes the bottleneck (multiple column cycles, large buffer requirements, long processing times) that occurs when the traditional Protein A process is matched with a high-titer harvest.

In the process development work described here, cell culture fluid containing ‘Antibody A’ that was harvested from a high-titer CHO process was concentrated and sent through a continuous bench-scale PEG/$ZnCl_2$ precipitation step. A subsequent downstream purification sequence consisting of four unit operations was developed to purify this

precipitated material. Following re-solubilization of the precipitate, the product stream was sent through a depth filtration sequence for clarification, anion exchange chromatography, cation exchange chromatography, and mixed-mode anion exchange/hydrophobic interaction chromatography. This purification process takes precipitated material and purifies it to the point where typical product and process-related impurities (host cell proteins, residual DNA, high molecular weight aggregates, residual PEG) are below industry expectations.

Concentrated mAb A harvest material was continuously precipitated utilizing a previously-developed PEG/$ZnCl_2$ precipitation procedure. This method takes advantage of the synergy gained when combining metal ion affinity precipitation (due to zinc chloride) and steric exclusion precipitation (due to PEG) to produce solid concentrated product-containing pellets which can be stored at -70 ^{O}C with no adverse effects to product stability. These pellets were thawed and re-solubilized with Histidine solution when ready for purification. Clarification of the re-solubilized precipitate was achieved by first diluting the material in low salt buffer (pH 6.5, 2.0 mS/cm), then sending the material through a C0HC and X0HC depth filter in series. The C0HC filter's large pore size (> 1.0 micron) helps to clear large insoluble species from the product stream, while the X0HC filter's smaller pore size (< 0.1 micron) and positively-charged media properties helped to eliminate smaller insoluble species and negatively-charged impurities.

Two methods of anion exchange purification were evaluated for the first column purification step. Traditional anion exchange column chromatography was compared to fast-flow anion exchange membrane purification for host cell protein reduction, DNA reduction, and overall step yield. Process material in low salt conditions (pH 6.5, 2.0 mS/cm) was used as load in both cases. Traditional AEX chromatography in flow-through mode

provided greater than 1 log clearance for both host cell protein and DNA, while retaining greater than 90% of mAb A product. The AEX membrane technology could not perform to this standard due to the low residence time of load material on the membrane. Screening of load pH and conductivity was performed to determine the optimal conditions for the second column operation, cation exchange chromatography in bind/elute mode. Results showed that pH 5.5, 5.0 mS/cm conditions were ideal for host cell protein clearance and yield. However, this condition caused a significant increase in product aggregation across the CEX step. Comparison of this condition to pH 4.6, 12.5 mS/cm run conditions previously optimized for mAb A capture from HCCF determined that the new condition was equally capable of high product yield but did not result in the aggregate increase seen previously.

Optimization of the final mixed-mode AEX/HIC flow-through column step, intended for aggregate clearance, was conducted using a high-throughput approach. A 2^3 factorial design of experiments was created that investigated the effect of pH, conductivity, and resin loading on yield of the mixed-mode step. Small-scale centri-columns were used for quick and rapid screening of the DOE conditions. Results of the DOE identified multiple promising run conditions, which were transitioned to lab-scale experiments in order to evaluate purification capabilities. This screening showed that pH 6.3, 200 mM NaCl, and 100 g/L resin loading conditions were appropriate for reducing the aggregate level of the product below 1.00% while still retaining 90% of product yield. Optimized mixed-mode conditions performed better in terms of yield and aggregate reduction than traditional HIC chromatography conditions used for mAb A.

A full process run was conducted, connecting all four clarification and purification steps together. Precipitated material was re-solubilized and sent through both depth filters, AEX in FT, CEX in bind/elute, and mixed-mode AEX/HIC in flow-through using the optimized

conditions developed for each step. Final process product characteristics showed that HCP and DNA levels were within acceptable limits recommended by the FDA. Final aggregate level was below the 1.00% specification set internally. Overall yield of the purification process was approximately 60%. A reversed-phase HPLC assay was developed in order to quantify the amount of free residual PEG in final process samples. Results showed that end-of-process PEG concentration was below the limit of quantitation of the assay (less than 2.5 ug/mL) and within typical industry specifications for free PEG.

The end result of the research described here is a process surrounding PEG/$ZnCl_2$ precipitation that can purify antibody product to within acceptable regulatory limits. Precipitation is a very useful technology because of its ability to decouple upstream and downstream processing while taking full advantage of the increase in productivity from high-titer cell culture processes. The optimized process developed here has proven it is capable of purifying precipitated antibody product to within acceptable impurity levels, highlighting its capability as a next-generation alternative to Protein A-based processes.

REFERENCES

[1] Wurm, F.M. (2004). Production of recombinant therapeutics in cultivated mammalian cells. *Nat. Biotechnology,* 22(11), 1393-1398

[2] Kelley, B. (2009). Industrialization of mAb production technology: The bioprocessing industry at a crossroads. *MAbs,* 1(5), 443-452

[3] McGlaughlin, M. S. (2010). An emerging answer to the downstream bottleneck. *BioProcess Int.*, 10, 58-61.

[4] Langer, E. (2013). Trends in Downstream Bioprocessing. *BioPharm International.* Retrieved from http://www.processdevelopmentforum.com/articles/trends-in-downstream-bioprocessing/1/

[5] Shukla, A.A., M. Etzel, and S. Gadam (2006). Process-scale bioseparations for the pharmaceutical industry, CRC Press, Boca Raton, FL.

[6] Kelley, B. (2007). Very large scale monoclonal antibody purification: the case for conventional unit operations. *Biotechnology progress*, 23(5), 995-1008.

[7] Adamson, S.R. "A new era in biotechnology," *BioProcess International Conference.* San Francisco, CA; 2006 November 6-9

[8] Arunakumari, A., J. Wang, and G. Ferreira (2007, February). Alternatives to Protein A: Improved downstream process design for human monoclonal antibody production. Supplement to *BioPharm International,* Retrieved from http://www.biopharminternational.com/biopharm/

[9] Jia Liu, J. (2009). Comparison of Camelid antibody ligand to Protein A for monoclonal antibody purification: A suitable alternative to Protein A chromatography. *BioPharm Int,* 22(9), 35-43

[10] Menegatti, S., Naik, A. D., & Carbonell, R. G. (2013). The hidden potential of small synthetic molecules and peptides as affinity ligands for bioseparations. *Pharmaceutical Bioprocessing*, 1(5), 467-485.

[11] Azevedo, A.M. et al. (2009). Partitioning of human antibodies in polyethylene glycol – sodium citrate aqueous two-phase systems. *Sep. Pur. Technology,* 65, 12-21

[12] Bradford, M.M (1976). Rapid, sensitive method for quantitation of microgram quantities of protein utilizing principle of protein-dye binding. *Anal. Biochem,* 7, 248-254

[13] Azevedo, A.M. et al. (2009), Affinity-enhanced purification of human antibodies by aqueous two-phase extraction. *Sep. Pur. Technology,* 65, 31-39

[14] Shukla, A.A. and J. Thommes (2010). Recent advances in large-scale production of monoclonal antibodies and related proteins. *Trends in Biotechnology*, 28(5), 253-261

[15] McDonald, P., Victa, C., Carter-Franklin, J. N., & Fahrner, R. (2009). Selective antibody precipitation using polyelectrolytes: a novel approach to the purification of monoclonal antibodies. *Biotechnology and bioengineering*, 102(4), 1141-1151.

[16] Mehta, A., Tse, M. L., Fogle, J., Len, A., Shrestha, R., Fontes, N., ... & Reis, R. V. (2008). Purifying therapeutic monoclonal antibodies. *Chemical Engineering Progress*, 104(5), S14.

[17] Yigzaw, Y., Piper, R., Tran, M., & Shukla, A. A. (2006). Exploitation of the adsorptive properties of depth filters for host cell protein removal during monoclonal antibody purification. *Biotechnology progress*, 22(1), 288-296.

[18] Curling, J. (2008) The Development of Antibody Purification Technologies, in Process Scale Purification of Antibodies (ed U. Gottschalk), John Wiley & Sons, Inc., Hoboken, NJ, USA.

[19] Iyer, H. V., & Przybycien, T. M. (1996). A model for metal affinity protein precipitation. *Journal of colloid and interface science*, 177(2), 391-400.

[20] Iyer, H. V., & Przybycien, T. M. (1995). Metal affinity protein precipitation: Effects of mixing, protein concentration, and modifiers on protein fractionation.*Biotechnology and bioengineering*, *48*(4), 324-332.

[21] Arakawa, T., & Timasheff, S. N. (1985). The stabilization of proteins by osmolytes. *Biophysical Journal*, *47*(3), 411-414.

[22] Bhat, R., & Timasheff, S. N. (1992). Steric exclusion is the principal source of the preferential hydration of proteins in the presence of polyethylene glycols.*Protein Science*, *1*(9), 1133-1143.

[23] Gronke, R.S., Jaquez, O. (2009). *US Patent Appication No. 12/425,328*. Washington, DC: U.S. Patent and Trademark Office.

[24] United States Food and Drug Administration. (1999). Guidance for industry: Q6B specifications: Test procedures and acceptance criteria for biotechnological / biological products. Rockville, MD.

[25] Champion, K., Madden, H., Dougherty, J., & Shacter, E. (2005). Defining your product profile and maintaining control over it, part 2. BioProcess Int, 3(8), 52-57.

[26] United States Food and Drug Administration. (1997). Points to consider in the manufacture and testing of monoclonal antibody products for human use. Rockville, MD.

[27] Cordoba-Rodriguez, R. V. (2008). Aggregates in MAbs and recombinant therapeutic proteins: a regulatory perspective. *BioPharm International,* 21(11).

[28] International Conference on Harmonization. (2006). Guideline Q3A: Impurities in new drug substances.

[29] Gagnon, P. (1996). Purification tools for monoclonal antibodies.

[30] Zhou, J. X., & Tressel, T. (2006). Basic Concepts in Q Membrane Chromatography for Large-Scale Antibody Production. *Biotechnology Progress*, 22(2), 341-349.

[31] Urmann, M., Graalfs, H., Joehnck, M., Jacob, L. R., & Frech, C. (2010). Cation-chromatography of monoclonal antibodies.

[32] Charles River Laboratories. (2012). Analytical Methods for Host Cell Proteins. Retrieved from http://www.criver.com/files/pdfs/.

[33] Wang, J. M., Diehl, T., Aguiar, D., Dai, X. P., & Arunakumari, A. (2009). Precipitation of process-derived impurities in non-Protein A purification schemes for antibodies.

[34] Romero, J., Chrostowski, J., de Vilmorin, P., & Case, J. (2006, November). Effects of pH and ionic conditions on microfiltration of mammalian cells: Combined permeate flux enhancement and mAb purification capabilities. In 2006 American Institute of Chemical Engineers Annual Meeting, San Francisco, CA

[35] Prashad, M., & Tarrach, K. (2006). Depth filtration: Cell clarification of bioreactor offloads. *Filtration & separation*, 43(7), 28-30.

[36] Schirmer, E. B., Kuczewski, M., Golden, K., Lain, B., Bragg, C., Chon, J., ... & Zarbis-Papastoitsis, G. (2010). Primary clarification of very high-density cell culture harvests by enhanced cell settling. *BioProcess Int*, 8(1), 32-39.

[37] Coffman, J. L., Kramarczyk, J. F., & Kelley, B. D. (2008). High-throughput screening of chromatographic separations: I. Method development and column modeling. *Biotechnology and bioengineering*, *100*(4), 605-618.

[38] Rathore, A. S., Joshi, V., & Yadav, N. (2013). Aggregation of monoclonal antibody products: Formation and removal. *BioPharm International*, 26(3), 40-45.

[39] Pall Corporation. (2013). Ion Exchange Membrane Devices. Retrieved from http://www.pall.com/main/laboratory/ion-exchange-membrane-devices-52121.page

[40] Knudsen, H. L., Fahrner, R. L., Xu, Y., Norling, L. A., & Blank, G. S. (2001). Membrane ion-exchange chromatography for process-scale antibody purification. *Journal of Chromatography A*, 907(1), 145-154.

[41] Tao, Y., Ibraheem, A., Conley, L., Cecchini, D., & Ghose, S. (2014). Evaluation of high-capacity cation exchange chromatography for direct capture of monoclonal antibodies from high-titer cell culture processes. *Biotechnology and bioengineering*.

[42] Gillespie, R., Nguyen, T., Macneil, S., Jones, L., Crampton, S., & Vunnum, S. (2012). Cation exchange surface-mediated denaturation of an aglycosylated immunoglobulin (IgG1). *Journal of Chromatography A*, *1251*, 101-110.

[43] Lu, Y., Williamson, B., & Gillespie, R. (2009). Recent advancement in application of hydrophobic interaction chromatography for aggregate removal in industrial purification process. *Current pharmaceutical biotechnology*, *10*(4), 427-433.

[44] Connell-Crowley, L., Larimore, E. A., & Gillespie, R. (2013). Using high throughput screening to define virus clearance by chromatography resins. *Biotechnology and bioengineering*, 110(7), 1984-1994.

[45] Ghose, S., Tao, Y., Conley, L., & Cecchini, D. (2013, September). Purification of monoclonal antibodies by hydrophobic interaction chromatography under no-salt conditions. In *MAbs* (Vol. 5, No. 5, p. 795). Landes Bioscience.

[46] IonSource Tutorial. (2001). Reversed-Phase HPLC Basics for LC/MS. Retrieved from http://www.ionsource.com/tutorial/chromatography/rphplc.htm

[47] Chen, J., Tetrault, J., Zhang, Y., Wasserman, A., Conley, G., DiLeo, & Ley, A. (2010). The distinctive separation attributes of mixed-mode resins and their application in monoclonal antibody downstream purification process. *Journal of Chromatography A*, 1217(2), 216-224.

[48] EMD Millipore. (2014). Viresolve Pro and Pro+ Solutions. Retrieved from http://www.millipore.com/catalogue/module/c74670

[49] Edwards, C.K., Martin, S.W., Seely, J., Kinstler, O., Buckel, S., Bendele, A.M., Cosenza, M.E., Feige, U. and Kohno, T. (2003). Design of PEGylated soluble tumour necrosis factor receptor type i (PEG STNF-RI) for chronic inflammatory diseases. *Advanced Drug Delivery Reviews,* 55 1315-1336.

[50] Moreadith, R. and Collen, D. (2003). Clinical development of PEGylated recombinant staphylokinase (PEG-SAK) for bolus thrombolytic treatment of patients with acute myocardial infarction. *Advanced Drug Delivery Reviews,* 55 1337-45.

[51] Arduini, R.M., Li, Z., Rapoza, A., Gronke, R., Hess, D.M., Wen, D., Miatkowski, K., Coots, C., Kaffashan, A. and Viseux, N. (2004). Expression, purification, and characterization of rat interferon-[beta], and preparation of an N-terminally PEGylated form with improved pharmacokinetic parameters. *Protein Expression and Purification,* 34(2), 229-242.

[52] Arpicco, S., Dosio, F., Bolognesi, A., Lubelli, C., Brusa, P., Stella, B., Ceruti, M. and Cattel, L. (2002). Novel poly(ethylene glycol) derivatives for preparation of ribosome-inactivating protein conjugates. *Bioconjugate Chemistry,* 13(4), 757-765.

[53] Nijs, M., Azarkan, M., Smolders, N., Brygier, J., Vincentelli, J., Vries, G.M.P., Duchateau, J. and Looze, Y. (1997). Preliminary characterization of bovine 38 beta-lactoglobulin after its conjugation to polyethylene glycol. *Biotechnology & Bioengineering,* 54(1), 40-49.

[54] Zhang, J. (2010). Manufacture of Mammalian Cell Biopharmaceuticals. Manual of Industrial Microbiology and Biotechnology, 3rd ed., R. Baltz et al.(eds.). ASM Press, Washington, DC. Chapter 13. pp. 179, 195.

[55] Curtis, S., Lee, K., Blank, G. S., Brorson, K., & Xu, Y. (2003). Generic/matrix evaluation of SV40 clearance by anion exchange chromatography in flow-through mode. *Biotechnology and bioengineering,* 84(2), 179-186.

[56] Miesegaes, G. R., Lute, S., Strauss, D. M., Read, E. K., Venkiteshwaran, A., Kreuzman, A., ... & Brorson, K. (2012). Monoclonal antibody capture and viral clearance by cation exchange chromatography. *Biotechnology and bioengineering*, 109(8), 2048-2058.

[57] Makowiecki, J., & Mallory, H. (2013). Adjusting pH During Viral Inactivation. *Genetic Engineering and Biotechnology News,* 33(8).